Article

A three degrees of freedom switchable impedance myoelectric prosthetic wrist

The International Journal of Robotics Research
2024, Vol. 43(11) 1649–1675
© The Author(s) 2024
Article reuse guidelines:
sagepub.com/journals-permissions
DOI: 10.1177/02783649241231298
journals.sagepub.com/home/ijr

Patricia Capsi-Morales[1], Cristina Piazza[1], Giorgio Grioli[2,3], Antonio Bicchi[2,3] and Manuel G. Catalano[3]

Abstract

Wrist mobility contributes significantly to the execution of upper limb motor tasks. Despite this, current prosthetic wrists are far less advanced than other artificial joints. Typically, prosthetic wrists offer limited degrees of freedom, if any, which forces users to execute compensatory movements during task performance. This addition increases weight and complexity, two unwelcome factors in upper limb prostheses. This article presents the design of a 3-degree-of-freedom friction-lockable prosthetic wrist actuated by a single motor. The design features adaptable behavior when unlocked, promoting a gentle interaction with the environment, and enables users to adjust the hand configuration during pre-grasping phases. The proposed system was tested, combined with a hand prosthesis, and compared to a commercial rotational wrist during the execution of functional movements. Experiments involved nine able-bodied subjects and one prosthesis user. Participants also performed the experiments with their biological wrist (the intact wrist for the prosthesis user) as a control. Results showed that the lockable wrist was used actively 20% more often than the commercial solution without compromising users' execution time. Interaction tests reveal that compensatory movements are reduced when using the proposed design, resulting in closer resemblance to the control wrist's performance. The average satisfaction and usability scores were significantly higher for the proposed wrist, indicating its potential acceptance. Finally, the system was validated in a set of activities of daily living performed by the prosthesis user. The study contributes to the development of more intuitive and adaptable prostheses that can improve the quality of life of amputees.

Keywords

Prosthetic wrist, switchable impedance, compensatory movements, adaptable behavior

Received 22 May 2023; Revised 16 November 2023; Accepted 20 November 2023
Senior Editor: Elena De Momi
Associate Editor: Raffaella Carloni

1. Introduction

The development of arm prostheses is one of the most fascinating and open challenges in rehabilitation engineering. The limited performance of both human–machine interfaces (Oskoei and Hu 2007; Schultz and Kuiken 2011) and mechatronic solutions restricts the effectiveness of state-of-the-art prostheses. The deficit of compact and light actuators, combined with design trade-offs concerning the desired performance, prehension capabilities, and anthropomorphism, results in a reduced set of movements that current prostheses can accomplish (Controzzi et al., 2014). Furthermore, voluntary control over independent signals on residual limbs is scarce, which restricts users to control only a few degrees of freedom (DoFs) in active prostheses. Recent developments in myoelectric control have delved into the management of multiple DoFs by employing more advanced algorithms and/or an increased number of surface (Chen et al., 2023; Nowak et al., 2022) or intramuscular (Smith et al., 2015) EMG sensors, which gather supplementary data.

Prostheses often oblige their users to perform unnatural compensatory movements to recover their range of motion (Stavdahl 2002), produce larger forces (Zinck 2008), and recuperate an acceptable level of smoothness, accuracy, and energy efficiency (Todorov 2004). These movements

[1]Department of Computer Engineering, School of Computation, Information and Technology, Technical University of Munich (TUM), Garching, Germany
[2]Centro di Ricercas "E. Piaggio", Universita di Pisa, Pisa, Italy
[3]Soft Robotics for Human Cooperation and Rehabilitation, Istituto Italiano di Tecnologia, Genoa, Italy

Corresponding author:
Patricia Capsi-Morales, Department of Computer Engineering, School of Computation, Information and Technology, Technical University of Munich (TUM), Boltzmannstr. 3, Garching 85748, Germany.
Email: patri.capsi@gmail.com

increase the discomfort experienced when using robotic aids, hindering their acceptance (Davidson 2002). Furthermore, they often result in residual limb pain, musculoskeletal stress, and overuse syndromes that can lead to injuries in the long run (Gambrell 2008; Kidd et al., 2000; Østlie et al., 2011).

Although significant technological advances have been made in the design of dexterous prosthetic hands (Capsi-Morales et al., 2021), relatively little attention has been given to replacements for proximal joints, such as the wrist. The human wrist is responsible for orienting the hand in space during grasping and manipulation tasks, with three degrees of DoFs enabling flexion/extension (F-E), abduction/adduction (A-A), and pronation/supination (P-S) (Moser et al., 2020). By adjusting the hand position in accordance with the object's shape and placement, the wrist plays a crucial role in executing these tasks (Figure 1). Montagnani et al. (2015) prove that a single DoF hand with wrist F-E allows functions comparable to a highly performant multi-DoF hand without a wrist. Besides, Kyberd (2012) suggests that an adaptive wrist with both compliant and rigid behaviors could benefit the user by alternating between featuring adaptability during the approach and stability during holding.

This paper presents the design of an innovative semi-active 3-DoF prosthetic wrist, which can switch between two states: (i) adaptable and (ii) fixed (or locked), through the use of only one motor. When unlocked, the wrist can be oriented in any configuration, featuring compliant behavior that favors the interaction with the environment. Contrary to other designs present in the literature (see details in Sec. 2), this solution permits the fixation of all 3 DoFs through a friction-lockable mechanism when a desired configuration is reached. The proposed design allows the physical adjustment of the prosthetic hand orientation (e.g., during the pre-grasping phase) and the regulation of its stiffness, based on a simple myoelectric control strategy. This prosthetic wrist aims to (i) reduce compensatory movements of proximal joints and (ii) facilitate the reach and holding phases of the grasp. Furthermore, this design lets us investigate the functional capabilities of a prosthetic wrist with an enlarged range of motion, specifically in tasks that require proper hand orientation. To do so, we compare the proposed design to a commercial pronation/supination rotator, which is the most common type of active wrist. The comparison uses time-based metrics, biomechanical measures, and self-evaluation surveys. The experimental evaluation combines each of the two wrists with the same prosthetic hand. We tested nine intact volunteers and one subject with a congenital malformation at the transradial level (Figure 2). Results proved the feasibility and potential of the proposed wrist.

(a) (b) (c) (d) (e)

Figure 1. Examples of human wrist configurations in common grasps: (a), (b) flexion, (c), (d) pronation and abduction, and (e) pronation and adduction.

(a) Cosmetic prosthesis (b) Proposed system

Figure 2. Prosthesis user wearing (a) her own esthetic prosthesis and (b) the proposed 3 DoFs wrist system.

2. State of the art

The wrist represents an essential constituent of the hand-arm system in humans, whether it is natural or artificial. Jacobs (1993) showed that passive prosthetic wrists improve the reaching and grasping abilities, substantially reducing or entirely preventing compensatory movements. Accordingly, the orthopedic prosthetics market offers several passive wrists, where the user manually adjusts the configuration of the wrist during or previous to task execution. Unfortunately, function of passive wrists is limited when manipulating with both hands (Sears et al., 2005). Looking for compliant wrists (Bajaj et al., 2015), the only few solutions available on the market offer 1-DoF (flexion/extension) or 2-DoFs (flexion/extension and abduction/adduction). Slightly more advanced solutions include compliant wrists that use torsional springs to hinder the movement when the hand grasps heavy objects. Finally, a spherical joint for children prostheses (MyolinoWrist, Ottobock) presents different levels of friction that the user can set manually for a continuous flexion of the hand. Alternatively, the orthopedic market features active solutions designed to improve arm dexterity. Unfortunately, those are still extremely basic and the user has to use non-intuitive switching control techniques to command one DoF at a time. The most common active wrist is a 1-DoF rotator module that restores the prono/supination movement. Metzger et al. (2012) proved that this restoration decreases the compensatory movements in transradial prosthesis users.

Even in research, there is modest progress in the field of prosthetic wrists design. The RIC Arm (Lenzi et al., 2016) uses active serial 2-DoF to impart pronation and flexion to the terminal device. The solution in Fite et al. (2008) presents a parallel 3-DoF gas-actuated architecture. Bajaj and Dollar (2018) presented an alternative composed by 2-DoFs parallel mechanism and a belt-driven serial mechanism for continuous pronation. Other solutions explore more compact and compliant structures with multiple DoFs (Demofonti et al., 2023; Lee et al., 2021). For a complete review, please refer to Bajaj et al. (2019). Research is also scant when looking at the issue of measuring the impact the wrist joint has on the overall capabilities of a prosthetic limb. Bertels et al. (2009) showed that coupling a conventional prosthetic hand with 1-DoF wrist reduces the extent of compensatory movements required to reach objects. Some studies compare the performance of stiff versus compliant wrists during Activities of Daily Living (ADLs) (Deijs et al., 2016; Deijs et al., 2016; Petersen 2008). Although both of these approaches have limitations, these studies show that the adaptive capabilities of compliant wrists improve the function of prostheses, especially in bimanual manipulation. Kyberd (2012) compares different wrists combined with a traditional 1-DoF hand. Results demonstrated that while stiff wrists force individuals to perform significant compensatory movements during the reaching phase, compliant wrists were unpractical while manipulating heavy objects.

Recent preliminary studies worked on the insertion of lockable passive wrists for prosthetic applications. Montagnani et al. (2013) presented a wrist prototype that exploits two polymeric elements as springs to select compliance and a bevel gear differential mechanism to orient the end effector in 2-DoFs. However, the stiffness selection was only possible with the wrist and hand axes in alignment, limiting the *stiff mode* only to holding objects straight. The same concept, adapted to hydraulically actuated body-powered hand prostheses, was presented in Montagnani et al. (2017). There, a unique master hydraulic cylinder drove the hand–wrist system. When the hand closes, the pressure of the hydraulic circuit changes to disable the flow in the wrist circuit through suitable valves, switching the wrist from free to locked in a certain configuration (continuous locking). The main drawback is the connection of both circuits, which does not allow independent control of the wrist and hand, limiting the wrist functionality to orienting for a better approach of the object. Likewise, Cappello et al. (2022) presented a 2-DoF wrist with a hemispherical unidirectional ratchet mechanism that automatically switches impedance when grasping and can completely lock only when the pin engages the central plughole at the rest position.

3. Friction-lockable wrist

3.1. Preliminary design considerations

We design a dexterous yet compact system for transradial prostheses that combines the benefits of compliant and rigid wrists. Our objective is to add 3 DoFs to the prosthetic limb to increase grasping dexterity and user's autonomy. That would let us study the impact that a larger range of motion have on the overall prosthetic functionality. Moreover, inspired by Kyberd (2012) and Montagnani et al. (2017), we include passive adaptability and switchable impedance. We believe those latter two features would let the user pre-orient the hand intuitively by exploiting the environment and in a more stable fashion.

Because of the wrist role in prehension, we require its control to be simple and independent of the hand. Therefore, the wrist mechanism should switch from an *adaptive state* to a *fixed* joint configuration by locking and unlocking. The control of the single discrete Degree of Actuation (DoA) for locking and unlocking should depend on a myoelectric control scheme that does not compromise the hand motions.

We foresee two main types of application scenarios. In the first scenario, the user reaches a light object taking advantage of the adaptable wrist behavior. Therefore, the wrist is adaptive during the reaching phase. Afterward, the wrist locks (if desired) to give support and precision during the holding phase. The second scenario accounts for those cases in which the preshaping of hand orientation is fundamental to ensure the success of the grasp. These latter

cases require the wrist rigidly fixed in the right position during reaching, to guide the approach to the object. The wrist stays locked during the holding phase as well.

To obtain a compact design of a 3-DoF joint lockable in all directions with only one actuator, we inspected several technologies in the literature. Nonetheless, a lot of the already existing options have issues with the size (Brown et al., 2010), the constant high power input requirements (Telleria et al., 2009), or exhibit a design that compromises our requirements (Palpacelli et al., 2014). Finally, the simplicity and compactness of a friction-lockable spherical joint for industrial applications (Alvin 2011) inspired our prototype design for a prosthetic wrist with switchable impedance properties.

3.2. Mechanical design

Figure 3 shows the proposed wrist design. Its general shape is cylindric for easy placement inside the prosthetic socket, aligned with the longitudinal forearm axis. The wrist consists of a spherical joint encased between two rings used to modulate the friction force on the sphere that constrains its rotation in the current orientation. A more detailed description on this concept and design is reported in Capsi-Morales et al. (2022).

One of the rings can move axially relative to the other one fixed to the socket interface **(a)**. This motion produces an opposable behavior that modulates the friction force applied to the spherical joint. A triangular cam disc **(c)** converts the rotational movement of the motor shaft **(j)** into the vertical displacement of the drivable ring **(b)**. Three vertical pins **(g)** guide the sliding of the drivable ring **(b)**. The sphere **(h)** interferes with the trajectory of the two rings and opposes their closing motion and, in turn, the rotation of the motor. This opposition lets the motor generate compression forces on the sphere and consequently modulates friction to switch the wrist impedance state.

The un-hindered displacement of the two rings would be ~1.5 mm, which is small compared to the sphere radius (10 mm). Therefore, we model the friction force generation mechanism as

$$F_{fric} = vF_{compr} = vK(\Delta_h) \tag{1}$$

where F_{fric} is the friction force, v is the friction coefficient, F_{compr} is the compression force, Δ_h is the vertical compression of the mechanism, and K is the equivalent stiffness of the whole mechanism.

A MAXON DC-X 22s 24 V motor drives the displacement h_t of the ring **(b)** through a triangular cam, to ensure a constant transmission ratio. Therefore, the vertical compression is

$$\Delta_h = h_t - h_{t_0} \tag{2}$$

The value h_{t_0} corresponds to the configuration of pure tangency between the rings and the sphere when there is no compression force. Figure 4(a) shows a scheme of the cam disk and the conversion from rotational to vertical movement. The un-hindered vertical displacement of the ring **(b)**, h_t, is defined as

$$h_t = b \cdot \tan(\alpha) \tag{3}$$

where α is the output angle of the vertical displacement h_t of the roller. Figure 4(b) shows the rotational movement of the motor axis and linear displacement of the roller projected on the horizontal plane, as

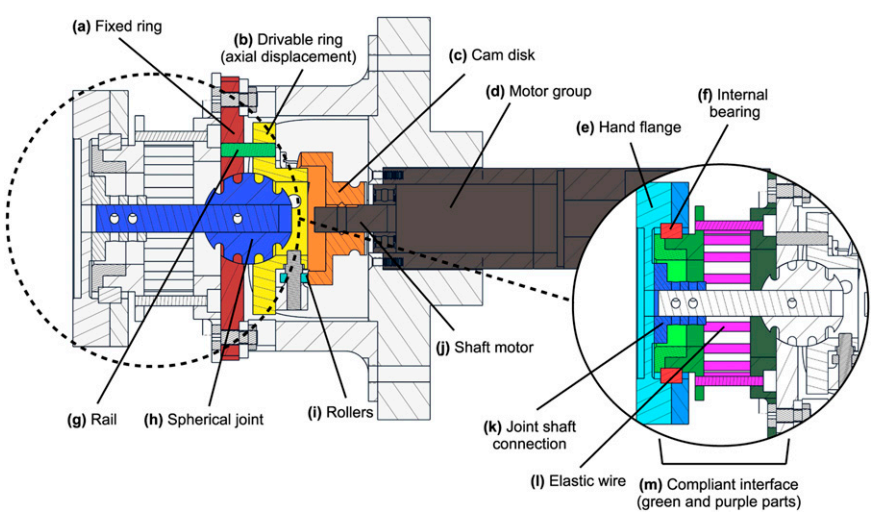

Figure 3. Mechatronic design of a 3-DoF wrist joint that can switch impedance in any configuration through just one motor. The circled section highlights the components from the compliant interface in flexion/extension and abduction/adduction together with the hand interface. The red bearing allows free pro/supination, while the pink elastic wires provide a natural interaction of the hand with the environment and humans.

$$b = c \cdot \tan(\varphi) \tag{4}$$

where c is the distance between the axis of the motor shaft **(j)** and the disk roller and φ is the output angle of the motor. The drivable ring applies pressure uniformly to the contact surface of the sphere.

The structure of the sphere **(h)** is not uniformly full but made of horizontal segments (see Figure 3 (h)). The space between them favors the deformation of the sphere, lowering the value of K. That reduces the sensitivity of F_{fric} with respect to the motor angle φ, in turn simplifying the system control.

We designed and manufactured the wrist and all the pieces needed to evaluate its performance with a prosthetic hand, including the prosthesis user's socket. Some of the most critical components are the sphere and the rings since they are always in contact and subject to high forces. Therefore, they are in aluminum. Other components that are subject to large forces are the cam disk and rollers. Therefore, the cam disk is in steel, and the rollers are in brass, impeding the plastic deformation of the rollers. The rest of the components are 3D printed in ABS plastic.

Table 1 resumes the main specifications of the implemented prototype. Please note that the goal of this prototype is to test the system's usability. Therefore, the dimension requirements of some components were not strict. For the moment, we report that the friction-locking capabilities were sufficient to maintain the hand in the desired configuration while grasping common objects and performing ADL. Optimizing the system to improve its wearability would require a fine analysis of the critical loads, which is out of the scope of this work. Based on the preliminary validation discussed in the rest of this manuscript, we will demand this for future work. Furthermore, note that this study lacks a detailed characterization of friction and impedance properties of the wrist mechanism. This was deliberate choice as our primary aim was to present a proof of concept and facilitate the initial testing of a higher DoFs prosthetic wrist with a simple control input. Therefore, detailed characterization of these properties fell outside the scope of this work.

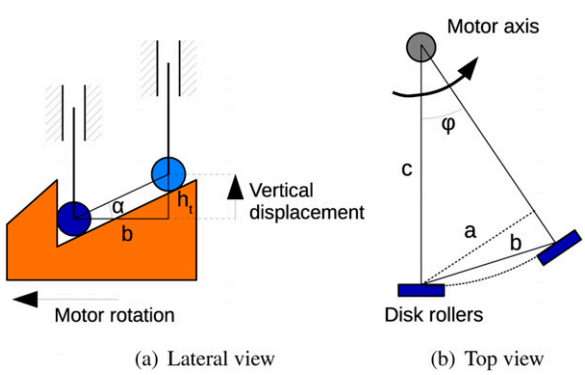

Figure 4. Geometric representation of the cam movement: Vertical displacement with a triangular cam shape (constant step) (a) and motor axis rotation (b).

3.2.1. Compliant interface. The final component of our wrist system is an elastic component placed in parallel to the spherical joint. Its function is to obtain a more natural appearance and interaction with the environment during the *adaptable state* (see Figure 5). This elastic component should provide the system with progressive compliance in F-E and A-A while leaving P-S motions practically free. The rationale for this selection is that the moment generated by the eccentricity of the Center of Mass (CoM) of the hand with respect to the P-S axis is typically smaller than around the other axes. Also, the P-S articulation represents a pivotal DoF in amputees to minimize compensatory movements (Bertels et al., 2009), which is often used at non-zero angles. For these reasons, and using indications from users in a preliminary design study which showed their preference for this solution, we preferred to introduce an adequate level of friction on the P-S articulation just to prevent unintended rotations, while we use a moderate elastic torque τ_k on the F-E and A-A axes. The compliant flange **(m)** in Figure 3, which lies between the fixed ring **(a)** and the hand frame **(e)**, implements this elastic component. A bearing **(f)** between the hand frame **(e)** and the output shaft **(k)** of the spherical joint allows hand rotation.

The mechanical response to F-E and A-A of the compliant flange **(m)** derives from a uniformly prestressed elastic wire **(l)** that connects the fixed ring **(a)** to the output shaft **(k)**. The compliant flange **(m)** defines the workspace of the end effector, its rest position, and the torque τ required to modify hand orientation when the wrist is in its *adaptable state* ($\tau > \tau_k$, Figure 5). Moreover, it also indirectly

Table 1. Specifications of the wrist prototype.

	System measures
Length (mm):	152.82
Length inside socket (mm):	120.39
Diameter (mm):	80
ROM F-E/A-A (°):	40 (from the vertical)
ROM P-S (°):	360
Wrist weight (g):	471
Estimated production cost (€):	800
Max. force to displacement (when locked, N):	20

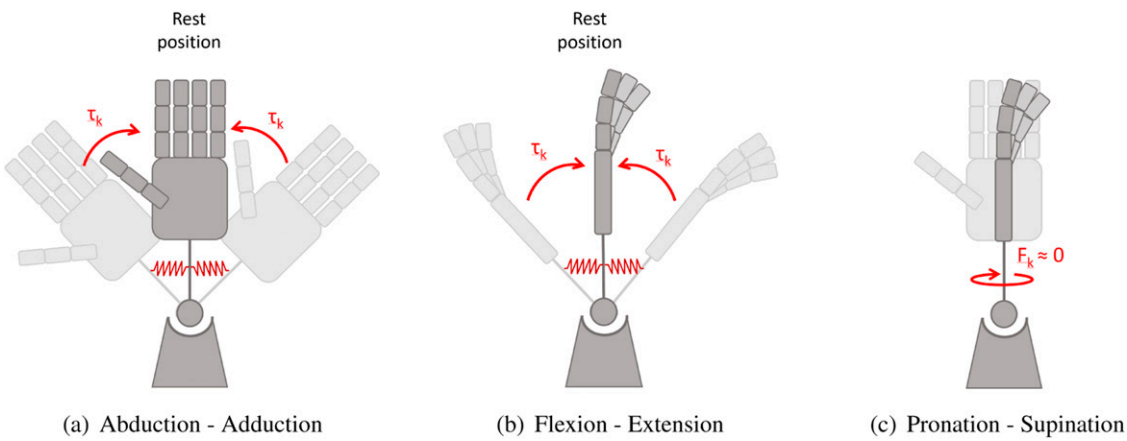

Figure 5. Adaptive behavior of the wrist on each DoF. τ_k refers to the pulling torque that the compliant interface exerts towards the longitudinal forearm axis. This position is termed as *rest position* of the hand and is defined by the alignment of the hand flange and the shaft of the motor. Note that for pronation–supination, the hand can rotate freely with $\tau_k \approx 0$. When the hand is grasping an object or interacting with the environment, the wrist can exhibit a different behavior only if $\tau_e > \tau_k$, where τ_e is the torque executed by the environment. Contrary to other lockable systems present in the literature, the proposed system can fix all DoFs at any configuration with only one motor.

influences the reaction force required to the motor to provide a successful locking. We sized the stiffness and preload of the elastic wire **(l)** experimentally by trial and error.

3.3. Control and electronics

A 12-bit resolution magnetic encoder (AS5045, AustriaMicrosystems) senses the cam disk rotation and feeds it to a custom electronic board (Della Santina et al., 2017). The board runs a PD (p = .03 and D = 0.2), with a current limit of 2000 mA, to regulate the cam disk rotation to an external reference value. The board is also in charge of reading two commercial sEMG sensors (13E200 = 60, OttobockGmbH, Germany), worn by the user to control the hand–wrist system. The board communicates (via USB serial port) to a PC running the external control loop described below in MATLAB Simulink (Mathworks, Inc).

We aim to evaluate the performance of the proposed wrist in combination with a prosthetic hand. Moreover, we want to compare its performance to that of the most common wrist used in the market, that is, a rotational prono/supination joint. Therefore, we use the same control strategy and hand prosthesis for both prosthetic solutions to highlight the differences only due to the mechanical capabilities of the wrist.

Control strategies adopted for multi-digit hands in the clinic (Cipriani et al., 2011; Dalley et al., 2009; Weir et al., 2008) and the market (Belter et al., 2013) were also used for hand–wrist combinations (Jiang et al. 2012, 2014; Piazza et al., 2020; Young et al., 2013). We adopt a control strategy commonly used in myoelectric prostheses consisting of a simple hand (1 DoA) and a rotational wrist (1 DoA). The strategy uses only two sEMG channels to control the direction of each DoA (wrist or hand). The choice between controlling the wrist or the hand depends on the velocity of the sEMG activation (e.g., four-channel control program [13E205 MyoRotronic, Ottobock]). As explained in the scheme in Figure 6(a), (a) slow activation sends the EMG proportionally commands to the hand velocity, while a fast activation goes to the wrist movement. The rationale behind this control modality being that fine grasping usually needs fine regulation of the hand position, therefore slowly increasing signals.

For the rotational prono/supination joint, the user controls the level of rotation, while for the proposed joint, a fast activation corresponds to the wrist locking. Figure 6(b) presents the Finite State Machine used. Although both robotic systems share the same control strategy, their different motion characteristics require a slightly different methodology to control each wrist. In the case of the rotational wrist, EMG_i controls the rotation speed of the wrist pronation/supination angle. The user should remain in *CW*/*CCWrot* state until reaching the desired orientation. In our prototype, an EMG impulse higher than Th_i locks the wrist in a certain orientation or unlocks it, depending on which EMG channel overcomes the threshold.

The states colored in red (Figure 6(b)) refer to wrist activations, and *SH* refers to the prosthetic hand used in the experiment. The *Stay* state maintains the position of each motor until the next change of state, while the two Sw_i states execute a timer to evaluate the subject intention (to activate the wrist or the hand, depending on the threshold of activation). The threshold of the wrist Th_{i_wrist} is larger than the hand one Th_{i_SH}, implying that fast activations are related to the wrist.

4. Experimental validation

We tested the proposed system functionality (hereafter termed lockable wrist—LW) and compared its performance with a prono/supination joint (rotational wrist—RW) and a control wrist (CW) for each participant. For the comparison,

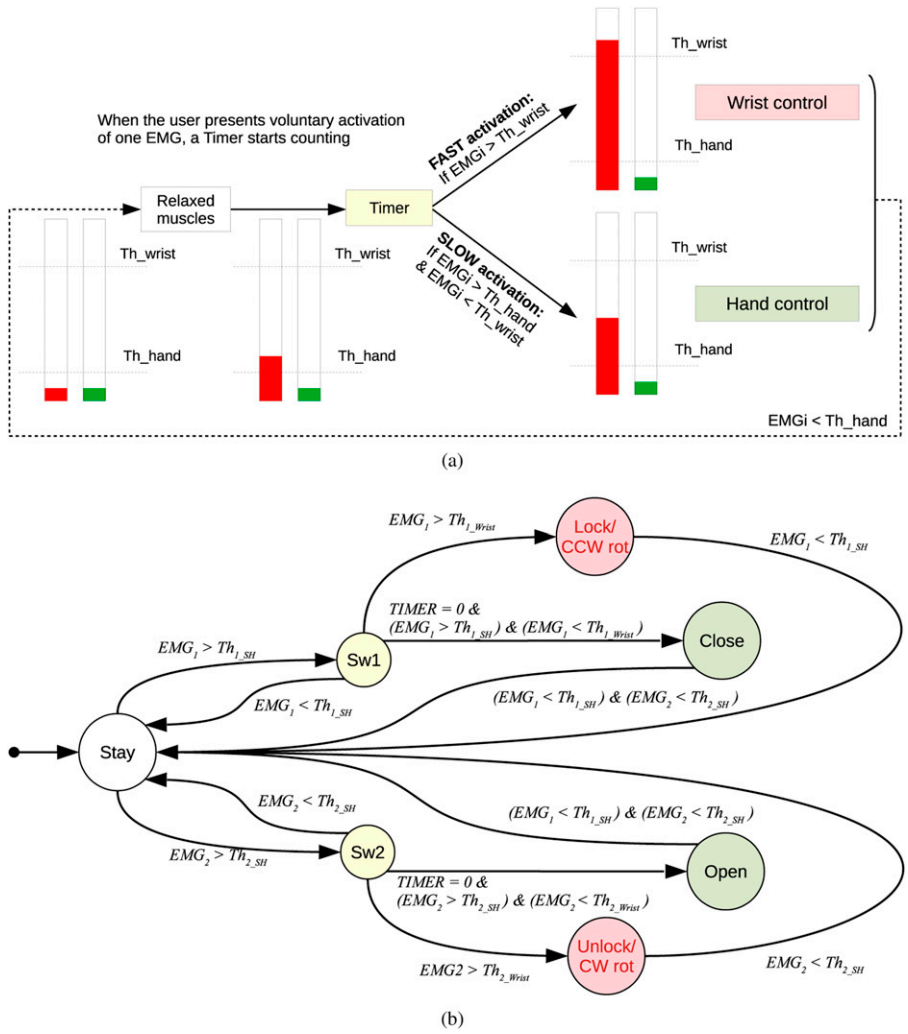

Figure 6. Control method: (a) presents a scheme of the rationale behind the control methodology. Here, we generalize with a unique threshold for each DoA, but this might change depending on the muscle properties of the subject and the algorithm implementation. (b) shows the implemented Finite State Machine that commands both hand and wrist movements.

we combined the two robotic wrists with the SoftHand Pro (SHP) prosthetic hand (Godfrey et al., 2018) using the control described in Sec. 3.3. Notably, also in the experiments with the control wrist, the able-bodied subjects used the SHP.

The experiment enrolled 10 participants: 9 able-bodied subjects (AB, 6 male and 3 female, 24–35 years old, 174.8±8.5 cm height) and 1 subject with a congenital malformation at the transradial level (left arm, female, 37 years old, 167 cm height). All of them gave their informed consent. Further details on the experimental setup, including the mechanical structure interfacing the different wrists and the prosthetic hand, are described later in Sec. 4.1.

To assess motor strategies used during movements, objective measures are necessary (de los Reyes-Guzmán et al., 2014). The reduction of compensatory motion of arm proximal joints is considered an objective measurement of the design success in new prosthetic devices (Metzger et al., 2012). Besides, the reduction of cognitive load or the intuitiveness required could be used for the same purpose. The latter is related to the timing, the willingness to use the additional feature, or may be evaluated through self-evaluation surveys from testers.

Upper extremity movements are classified into two big categories: functional movements and Activities of Daily Living (ADLs). For this reason, we designed two experiments to assess the performance of the different wrists under both the point of view of functional movement analysis and that of ADL. Table 2 resumes the overall experimental validation and the collected outcome measures. Fitts (1954) highlights the importance to quantify the task difficulty through movement amplitude and object size when testing a system. While experiment **(1)** permits the previous and a more quantified study of the mechanics of the motion, experiment **(2)** introduces the systems in practical actions. The functional movements of experiment **(1)** are replicable and consist of moving various objects at different heights. Sec. 4.2 reports the protocol details of the two experiments and the

Table 2. Overview of experimental validation. AB refers to able-bodied subjects and PU to prosthesis user.

Experiment	**(1)** Functional movements	**(2)** ADL
Wrists	LW, RW, and CW	LW, RW, and CW
Subjects	9 AB + 1 PU	1 PU
Metrics	Surveys (all), usage frequency (all), body motion analysis (AB only), and observations (PU only)	Additional observations

collected outcome measures. Additional observations from **(2)**, consisting of ADL, are reported in Sec. 6.2.1.

By using the switchable impedance wrist, we hypothesize that the hand can be oriented in a position closer to an unimpaired arm during the pre-grasping phase and thereby improve system user-friendliness. Furthermore, its compliance could enhance a soft interaction with target objects and its partly adjustment for a more stable grip.

4.1. Materials

4.1.1. Robotic devices. Figure 7(a) and (b) show the robotic hardware used for the experiments by the able-bodied subjects and the prosthetic user, respectively. Both hardware setups use the same prosthetic hand (SHP) in all conditions to separate possible effects due to the impact of the robotic hand from those due to the wrist design.

The device in Figure 7(a) is a non-invasive bypass system composed of a hand, one of the two wrists (LW or RW), a handle, an armrest, and a mechanical interface to connect to a gravity compensation device. The gravity compensator prevents the total weight of the system from hindering myoelectric control. An external battery of 24V is located outside and powers both the wrist and hand (12V). For the RW case, we used a custom 1-DoF rotational wrist. We recorded position data from its encoder during task execution. For able-bodied subjects, the left arm was chosen as it was the subject's non-dominant hand. This is considered appropriate as the majority of prosthesis users with a single loss use their prosthesis in a non-dominant manner, regardless of any natural dominance (Kyberd 2011).

Figure 7(b) presents the socket embedding the lockable wrist that interfaces with the prosthesis user residual limb. Two customized sockets were manufactured to integrate one of the two robotic wrists (LW or RW). Both solutions include the corresponding wrist, its attachment with the SHP, and two sEMG sensors attached to a compliant inner socket that accommodates the stump of the prosthesis user. At the moment, the electronic board that controls the LW is located outside the socket and interfaced at the arm level with a fan to avoid high temperatures near the stump for security reasons. For the prosthesis user, we used the Electric Wrist Rotator from Ottobock as RW because of its compact design and well-known acceptance.

In the control test, able-bodied subjects used their wrist to orient the end effector with a handle interface that commanded the hand level of closure. In this case, we did not use EMG signals because only the myoelectric control

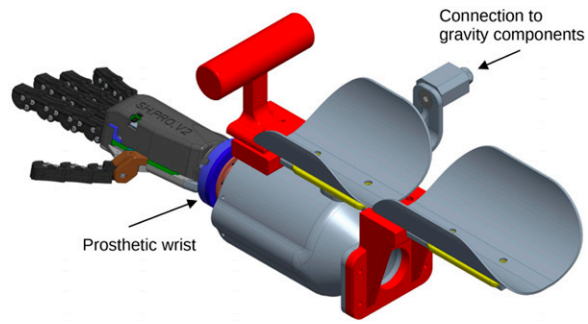

(a) Experimental setup used with able-bodied subjects

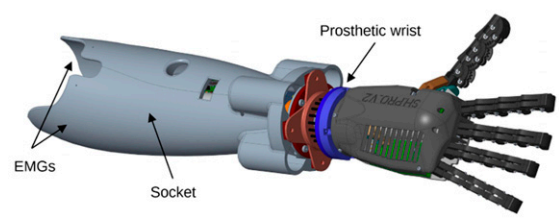

(b) Experimental setup used with the prosthesis user

Figure 7. (a) Extra arm attached to the gravity compensator for able-bodied experiments and (b) prosthetic interface: EMG, socket, and wrist–hand system. Both cases show the interface adapted for the LW, but the same setup was recreated for the RW.

of powered wrists is the scope of this paper. Accordingly, the gravity compensator is not present in this case, either in the prosthesis user's experiments (PU). The prosthesis user unimpaired arm (right) performed the experiment for the control test.

4.1.2. Measuring instruments. In experiment **(1)**, we used the Xsens System 3D motion tracking technology (Movella) to record the subjects' motions while performing the activities. The Xsens supplies MEMS-based inertial measurement units that provide the angles from the subjects' upper-body segments: trunk, shoulder, head, arm, and forearm. An image of the shelf containing the objects at the three height levels and the Xsens suit on one of the able-bodied subjects is shown in Figure 8.

Unfortunately, the electromagnetic interference from the actuators in the device of Figure 7(b) interferes with the Xsens calibration. The primary reason for the interference was the presence of the bypass interface. While all Xsens sensors could be placed directly on the skin of able-bodied

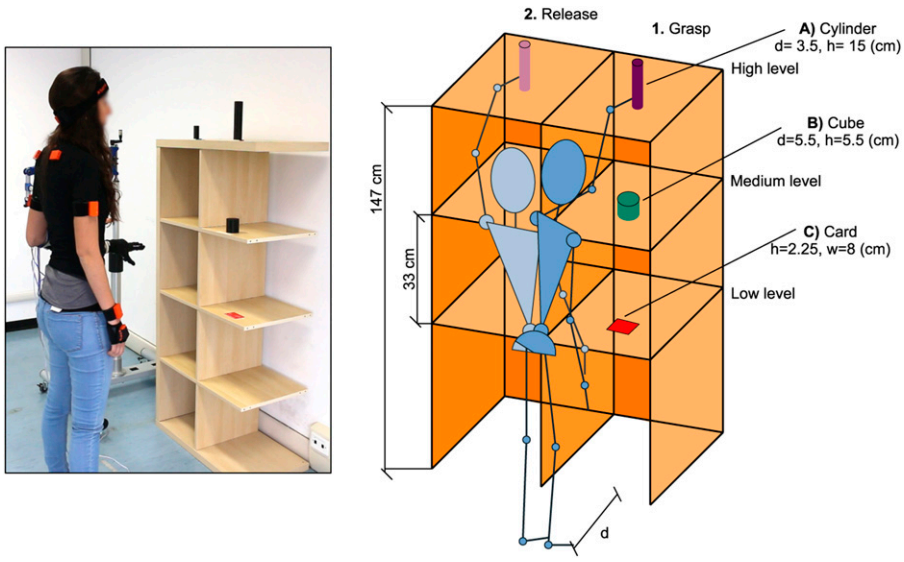

Figure 8. Sketch of the general setup of the experiment together with the object dimensions. On the left side, a picture of an able-bodied subject during the experiment. The right side presents an initial configuration of objects (1. Grasp). The final configuration (2. release) is reported with lighter colors.

participants, even when they used the bypass to hold the robotic system, prosthesis users had to position the sensors on their forearm and hand in proximity to the robotic system. This configuration led to electronic interference between the sensors and the robotic system during calibration and subsequent use. Despite various attempts to shield the electronics from sensor placement, it proved insufficient for reliable operation. Consequently, we decided against using Xsens with prosthesis users and instead utilized its data and experience as a qualitative complement of our study.

In experiment **(2),** videos were taken for PU while executing tasks with all wrists under study. A post hoc visualization of the data collected was done to report qualitative results regarding timing, natural body posture, and user's perception reported verbally during task execution.

4.1.3. Specimens. In experiment **(1)**, the subject grasps, transports, and releases one out of three objects on a shelf. Two of the three objects are cylinders of different sizes. One cylinder is thin and large, while the other has the same height and diameter. The third object is a card, which is usually considered a complex object in prosthetic manipulation because of its flat shape. According to the grasp taxonomy diagram proposed in Cutkosky (1989), the selected objects provide a good representation of grasps with (1) a long prismatic and (2) a compact circular power prehensile grasp, and (3) a compact circular precision grasp. Figure 8 shows the three objects with their dimensions.

Figure 8 shows a picture and a sketch of the shelf used, a standard IKEA KALLAX shelf. It has six slots on three different height levels used and two sides (left and right). As shown in Figure 8, a piece of paper-tape marks the position, on each of the three right shelves, where objects are initially placed. Objects must be released at the same height in the left side (no specific location).

All participants were positioned in front of the shelf at a fixed distance *d*. Nonetheless, due to the inevitable differences in the height among subjects, the distance of each shelf level relative to the subject varies on every occasion. After the completion of each grasping condition, subjects were instructed to return to the starting body position.

In experiment **(2)**, we instructed only the prosthetic user to perform a set of ADL. There were no strict instructions provided, except for specifying the starting location and posture for each activity. The participant had the freedom to perform the actions under its personal will and in a comfortable speed. The location of the camera respect to the area of interest for the execution of each action was marked in order to collect videos from a similar angle for each wrist tested.

4.2. Methods

4.2.1. Experimental protocol. A description of the overall experimental protocol for experiment **(1)** is presented in Table 3. To remove the operator's influence, each user performed all tasks with the three different wrists of study and the order of the two robotic solutions was randomized among subjects. Participants start performing the experiments using the control wrist (A) to get familiar with the different tasks involved. The first step for the evaluation of the prosthetic aids is the calibration phase (B), to set the maximum EMG amplitude and the activation threshold for each actuator suitable for each participant. Although the control strategy chosen is widely accepted in commercial devices because of its simplicity, a short training phase (C, J) is required to ensure satisfactory performance and avoid

Table 3. Protocol steps and expected duration.

Activity	Time expected (min)
(A) Experiment (Control wrist)	10
(B) System calibration	5
(C) Training (w1)	5
(D) Familiarization w1	10
(H) Experiment w1	20
(I) Rest time	5
(J) Training (w2)	5
(K) Familiarization w2	10
(L) Experiment w2	20
Total:	90

user's fatigue during testing. The biggest challenge in the control of LW is not to confuse hand aperture intentions with the wrist unlocking. Instead, in RW, proper control of wrist orientation is trained. After this process, subjects had 10 min to get familiar with wrist use (D, K) without specific instructions. Then, the experiment started (H, L).

Due to the difficulties of learning a more complex myoelectric control strategy, before starting with the experimental protocol, the PU tried and got familiar with the control strategy with no robotic system attached to her stump. Because of the difficulties of donning/doffing the system, we randomized only the order of the grasping conditions and the PU executed the protocol in the following order: the intact arm (CW) followed by the rotational one (RW) and finally, the lockable wrist (LW). We decided this order because, in case of fatigue, the results should affect the proposed system instead of deteriorating the PU experience with the commercial system.

The experiment **(1)** is a time-based protocol where subjects are required to complete the task in a standard velocity. Subjects are free to decide how to approach the target object and decide the use or not of the prosthetic wrist not to predetermine their possible compensatory movements. As in Carey et al. (2008), each grasping condition (3 heights × 3 objects = (9) was performed three times as a representative sample of subject motion without being affected by fatigue. The order of the grasping conditions performance was aleatory for each subject to avoid the interaction of a possible learning process. The use of the opposite (or intact hand) is just allowed during the pre-grasping phase, and only to change hand's orientation before fixing the lockable wrist (if necessary). Finally, three surveys were answered for each robotic wrist after the protocol was completed: (i) the System Usability Scale (SUS), (ii) a device satisfaction rank, and (iii) 16 additional custom questions regarding system performance. See their questions in Table 5, Table 6, and Table 7, respectively. The SUS and the 16 custom questions are 5-point Likert scales that go from *strongly disagree* to *strongly agree*. The device satisfaction is a 4-point Likert scale that goes from *very dissatisfied* to *very satisfied*. The SUS is a standard method to evaluate the usability and acceptability of a new system. Problems with system usability occur when a novel device obtains a score under 68 (average in the literature). With a score higher or equal to 80.3, it is considered that users completely accept the system.

The experiment **(2)** was performed only by the prosthesis user. We selected 12 daily life tasks to show functional improvement through the increase of wrist ROM and compliant behavior of the LW in more advanced activities. In this study, we focus on the reaching phase of the grasp, where we observe the feasibility of the task and if satisfactory, in which conditions. Qualitative results and general observations are reported in Sec. 6.2.1.

4.2.2. Performance metrics. Regarding the collected data from experiment **(1)**, functional movements, we identify as wrist activation any intentional or unintentional variation of the prosthetic wrist motor position, as recorded on its encoder. Therefore, we define *activation rate* as the average count of wrist activations across all tasks in experiment **(1)**. We define task *execution time* as the interval from when the experimenter verbally indicates the task starts to the successful release of the object. Note that a larger *activation rate* implies a larger use of the robotic device and a shorter time implies a faster execution of the task. Cases with a slower execution and higher range of *compensatory movements* are considered with poorer performance. An improvement in active device usage is attributed to a better upper extremity function within a given task or a reduction on the cognitive load to plan the desired grasping trajectory, as suggested in de los Reyes-Guzmán et al. (2014).

5. Results

This section presents the results from the functional movements test **(1)**, including the self-evaluation surveys.

We report Figure 9 to evaluate the impact of each wrist on functional movements through the average activation rate of each wrist during task performance (Figure 9(a)) and the average execution time (Figure 9(b)). Moreover, we also report the average task *execution time* limiting to the sole cases when wrists are activated (Figure 9(c)), to factor out the non-negligible activation time from the analysis. The main distinction between both time metrics lies in the analysis perspective. The general average execution time (termed *Execution time*) considers task completion, which may or may not involve active use of a robotic system. In contrast, the second metric (termed *Prosthetic aids in use*) focuses specifically on trials when the robotic system is actively engaged. This allows us to assess how the use of the robotic system impacts the execution time, particularly when the LW is used for configuration or stiffness switch, and when the RW is utilized for hand rotation.

We analyze Figures 10 and 11 to evaluate the impact of each wrist on functional movements through the compensatory motions of five body segment angles: Elbow flexion-extension, Shoulder flexion-extension, Shoulder adduction-abduction, Trunk adduction-abduction, and Trunk flexion-

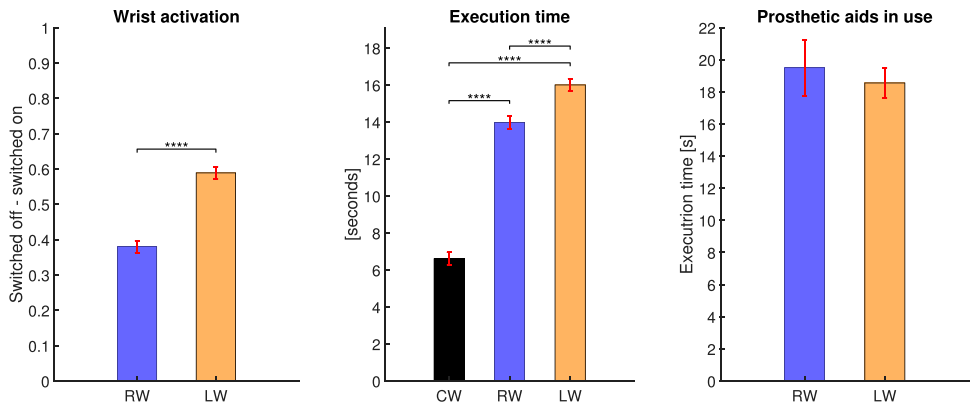

(a) $p < 0.0000$ (b) $p < 0.0000$ (c) $p = 0.6407$

Figure 9. Activation and execution time for all able-bodied subjects ($n = 9$). The black-dashed line divides the graph between the control wrist and the results with the prosthetic aids. The clear gray bar highlights the prosthetic wrist with better results for each aspect. Tukey–Kramer test significance is detailed with asterisks in the upper part of each graph. The estimated means for each wrist of study are presented with a bar plot, and the error bar refers to their standard error.

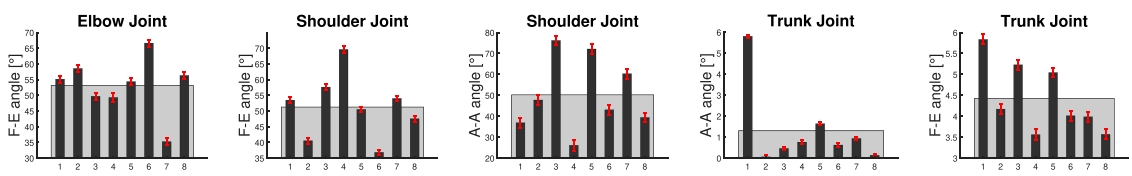

Figure 10. Subjects' means for each compensatory angle studied. The estimated mean for each subject is represented with a bar, together with its standard error. The average value is detailed in the background in a lighter color.

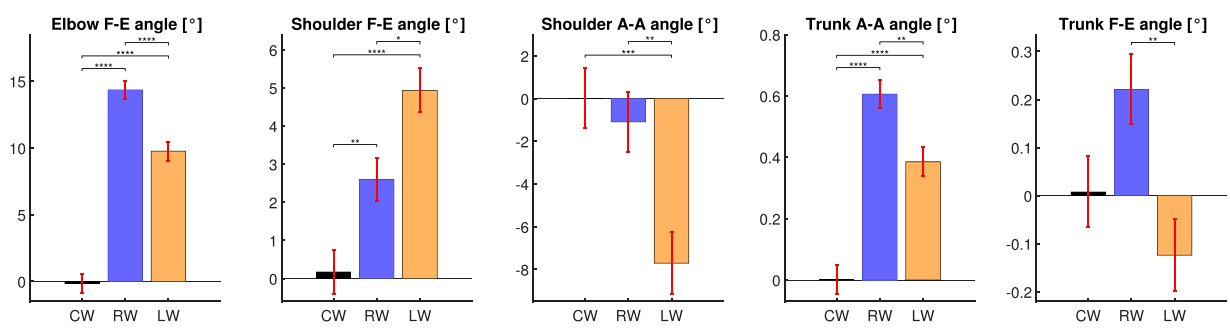

(a) $p < 0.0000$ (b) $p < 0.0000$ (c) $p = 0.0002$ (d) $p < 0.0000$ (e) $p = 0.0038$

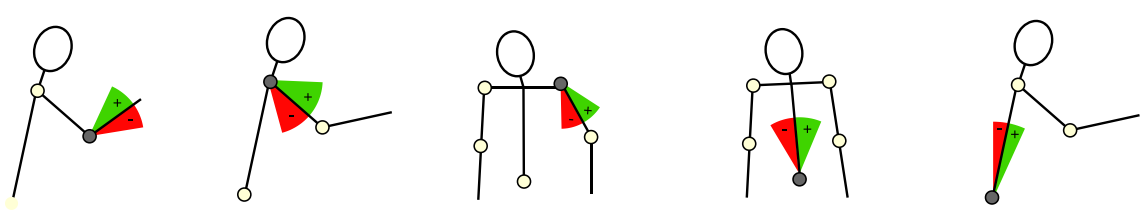

Figure 11. Compensatory movements from 5 body angles—subject's joint mean is removed to wrists comparable among subjects. A horizontal line in panels (a–e) indicates the neutral posture, which refers to each subject's average angle. A schematic body representation establishes the direction of compensatory movements with respect to each subject's average angle (neutral posture). The estimated means for each wrist of study are presented with a bar plot, and the error bar refers to their standard error. CW (control wrist) is the natural wrist of the subject. RW refers to rotational wrist and LW to the lockable wrist. We assume a robotic wrist obtains better results when performing less compensatory movements—giving the possibility to perform the task with a smaller workspace. The *p*-value from N-Way ANOVA is detailed in the caption. Significance from Tukey–Kramer—hsd post hoc test—is detailed with asterisks in the upper part of each graph.

extension. For those angles, Figure 10 reports the average values for each subject during the experiments (considering all trials). By subtracting an intra-subject average value (considering only trails with the control wrist), we define the compensatory movement angles (*compensatory movements*, for short), that we report in Figure 11. Moreover, for each of the previous figures, we report interaction analyses correlating *activation rates*, average *execution times*, and *compensatory angles* to the shape of the objects and their positions on the shelf (reported in Figures 12–18).

For the two prosthetic wrists, Table 4 reports categorical statistics on the wrist configuration used by the subjects to solve the "grasp" part of the task, as extracted by direct experiments observation. The possible categories are "no use," "Flexion-Extension only (F-E)," "only Prono-Supination for less than 45° (P-S 45°)," "only Prono-Supination between 45° and 90° (P-S 90°)," "Adduction-Abduction and Prono-Supination for less than 45° (P-S 45° + A-A)," and "Adduction-Abduction and Prono-Supination between 45° and 90° (P-S 90° + A-A)." Note that the same Table 4 also reports images and categories for the prosthesis user.

Finally, we report self-evaluation surveys handed out to participants. The surveys are (i) the System Usability Scale (Table 5), (ii) a Device Satisfaction rank (Table 6), and (iii) 16 custom questions on a Likert scale (Table 7). While beneficial for initial system validations, the absence of individuals with prostheses cannot be satisfactorily replaced with more able-bodied subjects. To emphasize the unique perspectives of prosthesis users, we report their answers separate from those of able-bodied subjects. Prosthesis

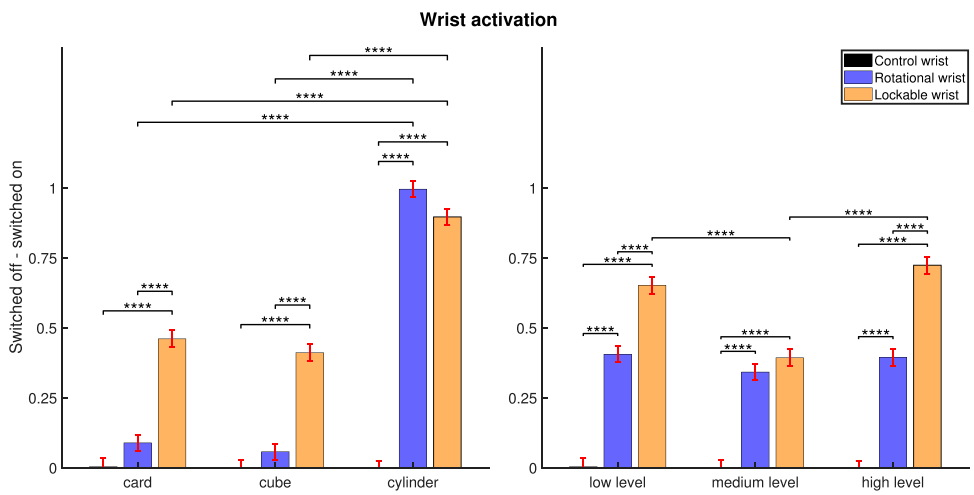

Figure 12. Interaction test for wrist activation. On the left side, there is the object-dependent wrist activation, while on the right side, results depend on the height. The left side shows the effect depending on the object: $p < .0000$ and the right side, depending on the height: $p < .0000$ (interaction p-value from N-Way ANOVA). Significance from Tukey–Kramer—hsd post hoc test—is detailed with asterisks in the upper part. The estimated means are presented with a bar plot, and the error bar refers to their standard error.

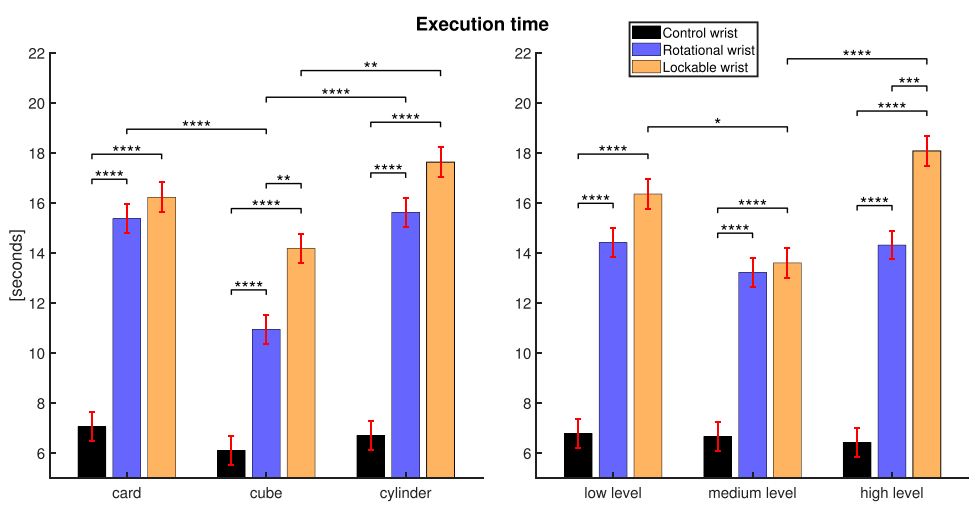

Figure 13. Interaction tests for execution time. The left side shows the results depending on the object: $p = .0028$ and the right side, depending on the height: $p = .0019$ (interaction p-value from N-Way ANOVA). Significance from Tukey–Kramer—hsd post hoc test—is detailed with asterisks in the upper part. The estimated means are presented with a bar plot, and the error bar refers to their standard error.

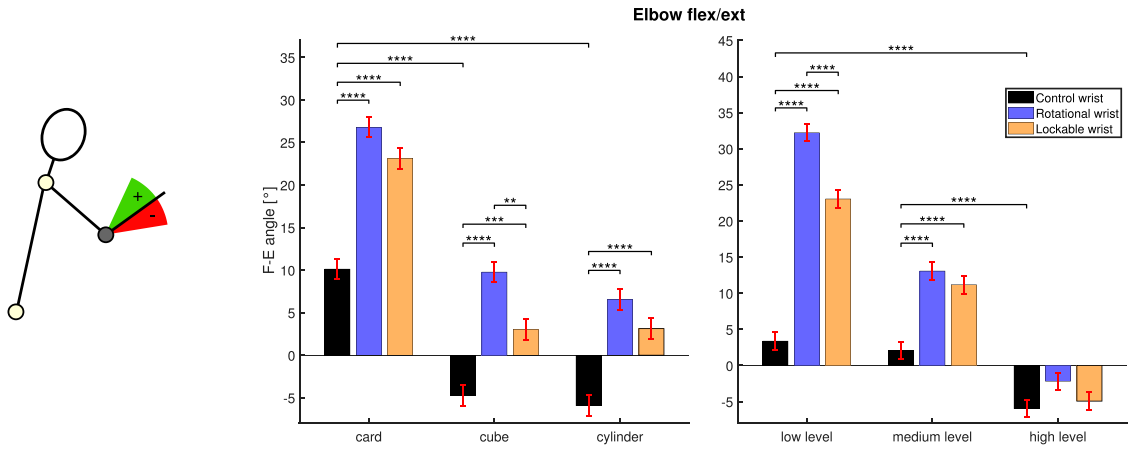

Figure 14. Interaction tests for elbow flex/ext. angle. The left side shows the effect depending on the object: $p = .1375$ and the right side, depending on the height: $p < .0000$ (interaction p-value from N-Way ANOVA). Significance from Tukey–Kramer—hsd post hoc test—is detailed with asterisks in the upper part. The estimated means are presented with a bar plot, and the error bar refers to their standard error.

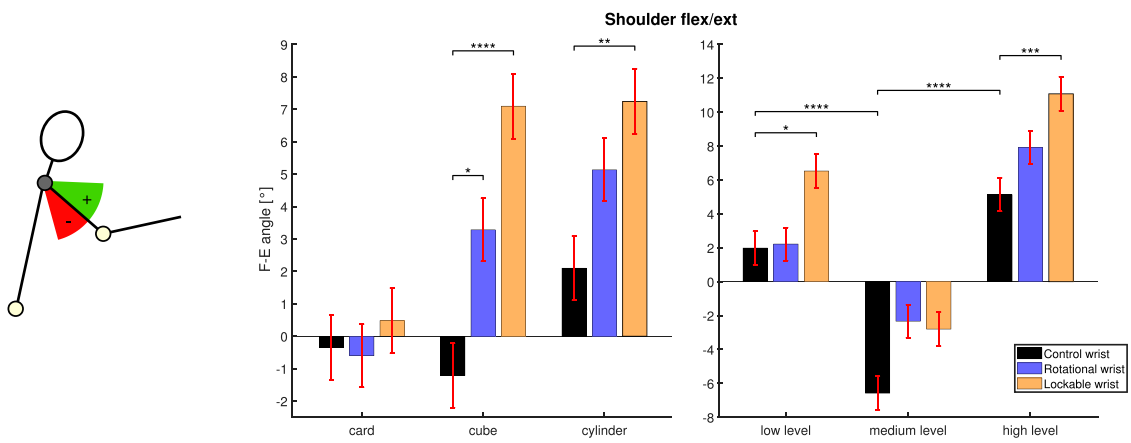

Figure 15. Interaction tests for shoulder flex/ext. angle. The left side shows the results depending on the object: $p = .0051$ and the right side, depending on the height: $p = .0972$ (interaction p-value from N-Way ANOVA). Significance from Tukey–Kramer—hsd post hoc test—is detailed with asterisks in the upper part. The estimated means are presented with a bar plot, and the error bar refers to their standard error.

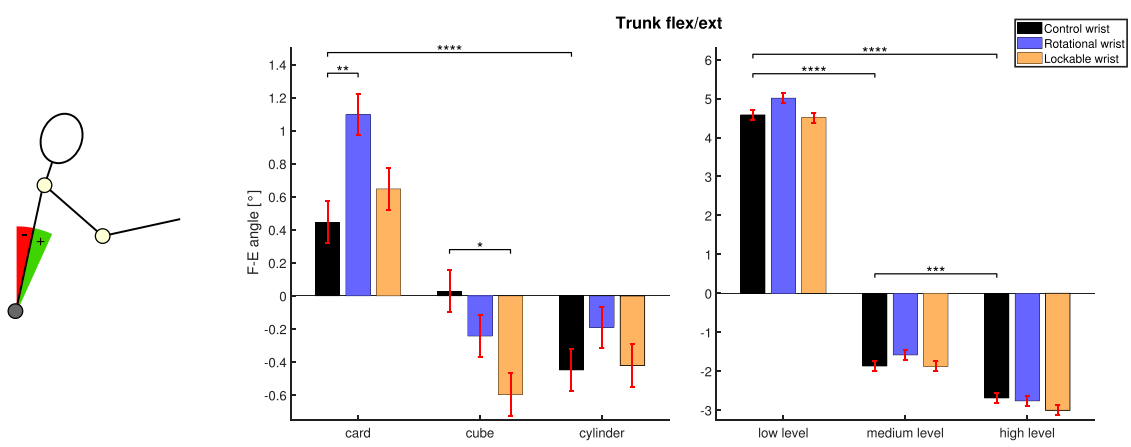

Figure 16. Interaction tests for trunk flex/ext. angle. The left side shows the results depending on the object: $p = .0019$ and the right side, depending on the height: $p = .3271$ (interaction p-value from N-Way ANOVA). Significance from Tukey–Kramer—hsd post hoc test—is detailed with asterisks in the upper part. The estimated means are presented with a bar plot, and the error bar refers to their standard error.

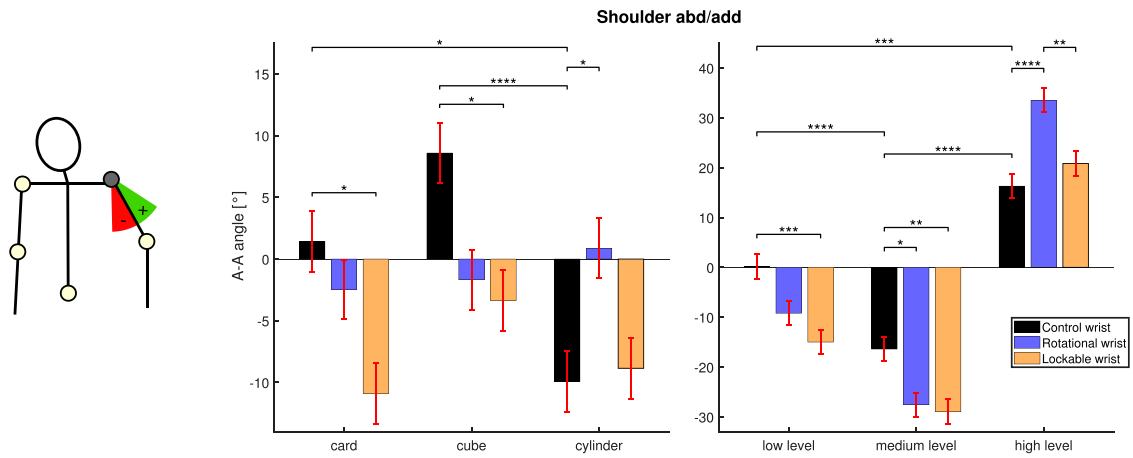

Figure 17. Interaction tests for shoulder abd/add. angle. The left side shows the results depending on the object: $p = .0003$ and the right side, depending on the wrist and height: $p < .0000$ (interaction p-value from N-Way ANOVA). Significance from Tukey–Kramer—hsd post hoc test—is detailed with asterisks in the upper part. The estimated means are presented with a bar plot, and the error bar refers to their standard error.

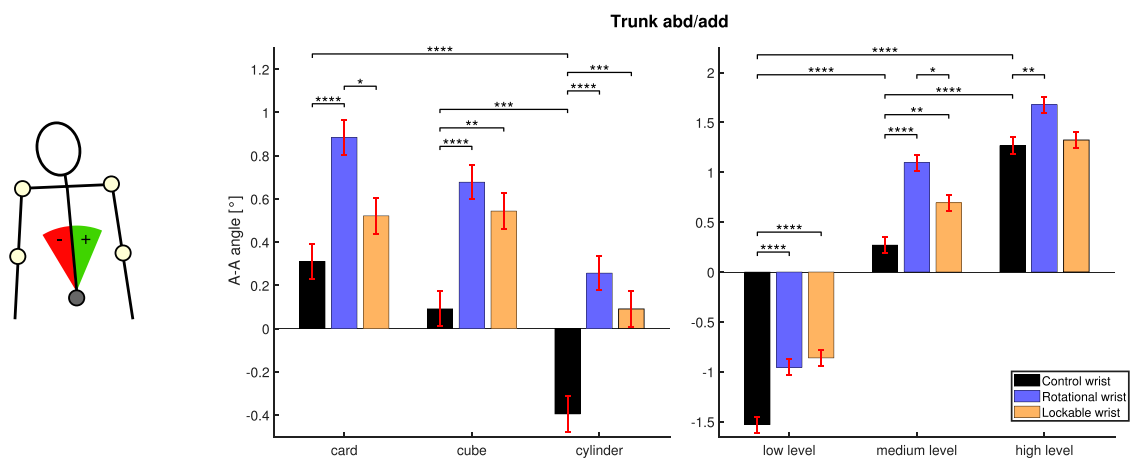

Figure 18. Interaction tests for trunk abd/add. angle. The left side shows the effect depending on the object: $p = .4052$ and the right side, depending on the height: $p = .0003$ (interaction p-value from N-Way ANOVA). Significance from Tukey–Kramer—hsd post hoc test—is detailed with asterisks in the upper part. The estimated means are presented with a bar plot, and the error bar refers to their standard error.

users' experiences with novel systems often differ to able-bodied subjects, and since they constitute a minority in our study, combining their responses with those of able-bodied participants could disproportionately weight the statistical results. However, for a more comprehensive overview, we have also reported the weighted response (considering both participant types) labeled as "All."

All data are processed, visualized, and statistically analyzed with MATLAB. Data are reported for each wrist type by indicating the initial letters: LW (Lockable wrist), RW (Rotational wrist), and CW (Control wrist). To reduce inter-subject variations, the two powered wrists are compared to each subject CW case. Results report the estimated means after an N-way ANOVA test, unless another test is explicitly mentioned, and represented in a bar plot, where the error bars refer to their standard error. The p-values are detailed in the caption of the corresponding figures. Significance from a Tukey–Kramer, also known as hsd post hoc test, is detailed through asterisks between compared couples when significant.

5.1. Able-bodied subjects

5.1.1. Functional movements. The activation rate and execution time for all able-bodied subjects ($n = 9$) are presented in Figure 9.

We observe that the LW presents a larger activation rate (+20%) than the RW, showing the interest of the participants in using the proposed system (Figure 9(a)). Activating either of the two wrists, the user positions the prosthetic hand for (a more comfortable) grasping action, which affects the total execution time. Indeed, the RW performed 2s faster than the LW (Figure 9(b)). Nonetheless, we observe no significant

Table 4. Approaching decision: Resumes how subjects decide to grasp each object depending on the condition and the system used. A color legend at the end of the table informs about the DoFs voluntarily used during the pre-grasping phase.

		Able-bodied subjects		Prosthesis user		
		Rotational wrist	Lockable wrist	Control wrist	Rotational wrist	Lockable wrist
CARD	High		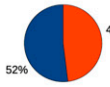	Top grasp + F-E+ A-A	Top grasp	Top grasp + F-E
	Medium			Top grasp + F-E	Top grasp	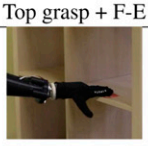 Top grasp + F-E
	Low		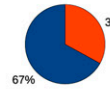	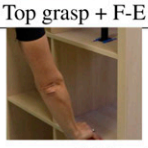 Top grasp + F-E + A-A	Top grasp	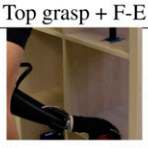 Top grasp + F-E
CUBE	High		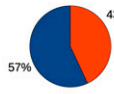	P-S 45° + A-A +F-E	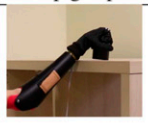 Top grasp	Top grasp + F-E
	Medium			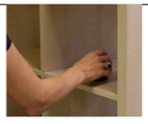 P-S 45°	Top grasp	Top grasp
	Low		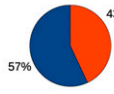	P-S 45° + A-A + F-E	Top grasp	Top grasp + F-E
CYLINDER	High	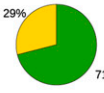	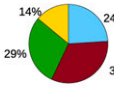	P-S 45° + F-E	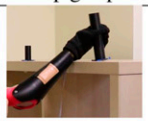 P-S 45°	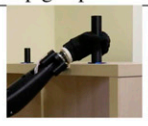 P-S 45° + A-A
	Medium	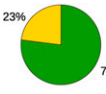	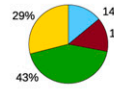	P-S 45° + A-A + F-E	P-S 45°	P-S 45° + A-A + F-E
	Low	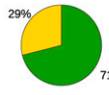	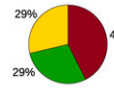	P-S 45° + A-A + F-E	P-S 45°	P-S 45° + A-A

No use · F-E · P-S 45° · P-S 90° · P-S 90° + A-A · P-S 45° + A-A

differences in execution time (p = .6407) if averaging only across those cases when both prosthetic aids were used actively (Figure 9(c)). That suggests that the observed 2s difference does not come from the LW performing worse time-wise.

Figure 10 reports the average values of the five body angles analyzed for compensatory motions. The conspicuous inter-subject differences confirm the heavy dependence of the final body configuration on the subject's physical features and personal preferences. Therefore, we

Table 5. System usability scale (SUS). Cells in green highlight answers with better score, while the yellow ones represent an equal result between prostheses.

	Able-bodied subjects			Prosthesis user		All	
	RW	**LW**	**p**	**RW**	**LW**	**RW**	**LW**
Q1. I think that I would like to use this system frequently.	2.75	3.88	0.0253 *	1	3	2.58	3.79
Q2. I found the system unnecessarily complex.	2.25	1.63	0.0455 *	4	1	2.43	1.57
Q3. I thought the system was easy to use.	3.56	4.11	0.0455 *	1	4	3.30	4.10
Q4. I think that I would need the support of a technical person to be able to use this system.	1.89	1.56	0.0833	4	4	2.10	1.80
Q5. I found the various functions in this system were well integrated.	3.44	4.11	0.0253 *	2	2	3.30	3.90
Q6. I thought there was too much inconsistency in this system.	2.33	1.78	0.0455 *	3	1	2.40	1.70
Q7. I would imagine that most people would learn to use this system very quickly.	3.56	3.88	0.0455 *	2	3	3.40	3.79
Q8. I found the system very cumbersome to use.	2.44	2.22	0.3173	4	4	2.60	2.40
Q9. I felt very confident using the system.	2.60	3.80	0.0833	1	2	2.44	3.62
Q10. I needed to learn a lot of things before I could get going with this system.	2.11	1.89	0.1573	4	3	2.30	2.00
SUS score (Wilcoxon signed-rank test - continuous data)	**59.17**	**71.11**	**0.0313 ***	**20.00**	**52.50**	**55.25**	**69.25**

Table 6. Device satisfaction (very dissatisfied–very satisfied). Cells in green highlight answers with better score, while the yellow ones represent an equal result between prostheses.

	Able-bodied subjects			Prosthesis user		All	
Features	**RW**	**LW**	**p**	**RW**	**LW**	**RW**	**LW**
Usefulness	3.00	3.33	0.0833	1	3	2.8	3.30
Training time	3.22	3.33	0.3173	1	3	3.00	3.30
Easy-to-use	2.89	3.44	0.1797	1	3	2.70	3.40
Grasp naturalness	2.56	3.11	0.1797	2	4	2.50	3.20
Comfort	2.89	3.11	0.3173	1	2	2.70	3.00
Level of fatigue	3.11	3.11	1	1	2	2.99	3.00
Overall satisfaction	3.00	3.22	0.1573	1	3	2.8	3.20
Average Satisfaction - Wilcoxon signed-rank	**31.75**	**41.27**	**0.0469 ***	**4.76**	**61.90**	**29.05**	**43.33**

define compensatory movement angles by subtraction, joint by joint, from the average angle of each subject across trials performed only with the control wrist. Note that even when using the control wrist, participants wear a bypass to execute the tasks with the same end-effector, which may influence the naturalness of their grasping body posture. For this reason, the method previously described assumes that the body postures for the control wrist are relatively more natural than the robotic wrists but not necessarily ideal. The resulting data (see, e.g., Figure 11) highlights the effects of each wrist in a more comparable way across subjects. Deviations from this intra-subject average posture were quantified as body compensations. Larger deviations indicate greater limitations imposed by the prosthetic device (or bypass), resulting in a less comfortable posture and, therefore, a worst wrist function. This approach was chosen due to the diverse configurations of the prosthetic devices respect to the control wrist case, variability among subjects' choices, and the need for a standardized reference point. Figure 11 proves that the LW obtains significantly smaller values than the RW for all angles except for the Shoulder joint. Note that, to get a more straighten arm, desired for a reaching phase, we expect smaller Elbow F-E and bigger Shoulder F-E angles. This combination occurs for the LW. Furthermore, a more negative Shoulder A-A angle indicates a more proximal location of the arm, also desired for comfort.

We report the analysis of the interaction between wrist types and grasped objects, and between wrist types and height levels. Although we show graphs from all measurements, we only discuss observations concerning those tests that obtained a significant p-value at an N-Way ANOVA, indicating significant differences among groups of the corresponding factor.

In the context of this study, robotic wrists interface with able-bodied participants via a bypass below the arm, which connects to the gravity compensation device. This interface configuration can potentially influence trajectory decisions when compared to scenarios involving prosthesis users, where wrist interfaces directly at the socket level. While one might expect able-bodied subjects to perform control actions comfortably, note that our approach considers the

Table 7. Likert-scale questions (strongly disagree–strongly agree). Cells in green highlight answers with better score, while the yellow ones represent an equal result between prostheses.

	Able-bodied subjects			Prosthesis user		All	
Questions:	**RW**	**LW**	**p**	**RW**	**LW**	**RW**	**LW**
Q1. It is comfortable to use the wrist in order to orient the hand.	3.44	4.33	0.0253 *	1	5	3.20	4.40
Q2. The movement / locking of the wrist is not fast enough.	2.33	2.56	1	3	2	2.40	2.50
Q3. I feel that I am not performing compensatory movements to execute the grasping action.	2.00	3.00	0.0455 *	2	4	2.00	3.1
Q4. It is simpler to move my body to reach the target object than changing the configuration of the wrist.	2.56	2.56	1	4	2	2.70	2.50
Q5. I complete the tasks in a short time.	2.89	3.78	0.0455 *	1	4	2.70	3.80
Q6. I feel limited in movement when performing the tasks.	3.33	2.56	0.1797	4	2	3.40	2.50
Q7. I do not feel tired after completing the experiment.	4.22	3.89	0.0833	2	4	4.00	3.90
Q8. It is more comfortable to grasp the object with compensatory movements than changing the configuration of the wrist.	2.44	2.44	0.4142	4	2	2.60	2.40
Q9. The wrist moves / locks fast enough.	3.75	4.25	0.0455 *	3	5	3.68	4.33
Q10. It is uncomfortable to use the wrist to orient the hand.	2.75	1.88	0.0455 *	4	1	2.88	1.79
Q11. I feel that I am doing a lot of compensatory movements to execute the grasping action.	3.38	2.50	0.0455 *	3	2	3.34	2.45
Q12. It is simpler to change the configuration of the wrist than moving my body to reach the target object.	3.50	3.63	0.5637	2	4	3.35	3.67
Q13. I feel tired after completing the experiment.	2.25	2.25	0.5637	4	2	2.43	2.23
Q14. It is more comfortable to change the configuration of the wrist than grasping the object with compensatory movements.	3.75	3.88	0.3173	2	4	3.58	3.89
Q15. I complete the tasks in a long time.	2.75	2.00	0.0833	4	2	2.88	2.00
Q16. I feel free in movement when performing the tasks.	2.63	3.38	0.0455 *	2	4	2.57	3.44

average joint angles across various tasks using only the control wrist, each task involving multiple objects and differing shelf levels. This approach allows us to assess the relative comfort levels associated with specific wrist configurations, including for the control wrist. For instance, we can discern that grasping objects on higher shelves or handling cylindrical objects may necessitate more body compensation than tasks involving simpler objects such as a box at mid-level shelves. By using this metric, we can effectively compare body compensations both within and across different wrist solutions.

Figure 12 shows the interaction tests for wrist activation rates. On the left side, we observe that participants use the LW significantly more often than the RW when grasping the *card* and *cube*, while in the case of the *cylinder*, both devices are actively used, at least for prono/supination movements. On the right side, results show that LW is used significantly more often than RW at the *low* and *high level*, that is, at the extreme conditions. Note also that there is no intra-RW difference corresponding to heights, while the LW presents a clear difference in usage at the *medium level*.

Figure 13 shows interaction tests about the task execution time. The first observations that we report are that the CW is significantly different from both prosthetic aids and that there are no differences among the diverse CW cases, that is, no intra-CW differences. Moreover, on the left side of Figure 13, we see that although the LW is slower than the RW for all objects, we find a significant difference only for the *cube*, suggesting the inconvenience in the active use of the LW to modify the wrist configuration only for this object. Note that RW and LW perform similarly for the *card*. However, while the LW is used in 50% of the occasions (see the left side of Figure 12), the RW is not intentionally used for this object. That suggests that LW improves the grasping of flat objects so much to recover the loss due to the time spent activating and orienting the wrist. Regarding height-dependent results, on the right side of Figure 13, even though generally LW > RW, data are only significantly different for the *high level*. No intra-RW significant differences are present for heights, which suggests that the decision making to prono/supinate the hand could be based on the object shape mostly. Both LW *low* and *high level* are significantly different from LW *medium level* because subjects used the LW more actively in these two levels (see the right side in Figure 12).

Figures 14–18 report the interaction tests concerning the five body angles studied to evaluate the reduction of compensatory movements with respect to the same two factors: object shape and height level. First, we present three angles that move in the sagittal plane. In the elbow flex/ext. angle, the right side of Figure 14 shows that there is consistency among wrist types, increasing the difference between CW and the robotic aids the lower is the height level. Although generally LW < RW, for a more straighten arm position, we have significance only at the *low level*, where RW also presents a more unnatural configuration

(i.e., largest differences between CW and RW). Concerning the shoulder flex/ext. angle, the left side of Figure 15 proves that despite RW < LW, there is no significant difference in any condition. Furthermore, there are no significance intra-CW results among objects, suggesting that there were no different experimental requirements concerning this angle. The trunk flex/ext. angle presents significance in the interaction with objects (left side of Figure 16). There is intra-CW significance between the *card* and the *cylinder*, which highlights different requirements in the definition of the experimental protocol regarding the morphology of the objects. For all objects, LW < RW, which indicates a more straight body posture, but without statistical significance. The trunk flex/ext. angle is mostly affected by the *card*, due to the difficulties encountered in grasping flat objects. In this case, the RW resulted significantly higher than the CW, suggesting that a more natural posture is possible with the LW.

In regards to the frontal plane, results from the shoulder abd/add. angle are influenced by both the object and the height level (see Figure 17). No statistical object-dependent difference between robotic aids occurs, even though the LW presents "better" results (i.e., closer to a stand straight up position and the arm more proximal to the trunk) in all conditions. For the *cube*, where the LW is not actively used, the difference between robotic solutions is very small. Instead, in the *cylinder*, the LW is similar to CW, while the RW is significantly higher than CW. There is an intra-CW statistical difference among height levels, which validates the existence of diverse requirements from the experimental protocol affecting this angle. Shoulder abd/add. angle is largely affected at the *high level* (with positive values respect to the intra-subject average), where LW is significantly lower than RW. There, the LW resulted in a much closer position to the natural one, that is, CW presents significant difference only with RW. Results from the trunk abd/add. angle are influenced only from the height level with significance between robotic aids at the *medium level* and with LW < RW (see right side of Figure 18). Moreover, the LW presents similar results to the CW at the *high level*, where CW is statistically lower only than RW.

Finally, the wrist configurations used for each experimental condition are observed and reported in Table 4, in terms of the desired approach directions and DoFs used. The first two columns report the usage percentage of each prosthetic wrist for able-bodied subjects after the visual inspection of the video footage. We observe that able-bodied subjects used the RW only to grasp the *cylinder*, regardless of the height. Participants performed grasps in two types of configurations for the RW, related only to the P-S; lateral grasp at 90°, or lateral grasp at 45°. On the contrary, the LW was used for all objects at certain height conditions. The LW was not intentionally used only for the *card* and *cube* at the *medium level*. Some participants used F-E motion to improve the grasp of these objects in extreme cases, that is, *low* and *high* heights. This use could depend on the height of the subject and users' expertise in controlling the device. In the case of the *cylinder*, the LW was used in 100% of the cases with different approaches. P-S motion was used to modify hand configuration at 45° or 90°, similar to the ones used for the RW. Besides, some participants explored a combination of P-S with A-A to facilitate the grasp depending on the height level. The percentage of combined approaches is lower in the *medium level* with 30%. Instead, in the *high level*, subjects profited more from combinations of P-S and A-A with its choice in more than 50% of the occasions.

5.1.2. Self-evaluation. We measure subjects' experiences through three different questionnaires. The average responses from able-bodied subjects, together with the *p*-value from the chi-square statistic, are used to prove statistical significance between prosthetic wrists after a Friedman's test (dependent categorical variables) applied to each question included: the System Usability Scale (Table 5), a device satisfaction rank (Table 6), and 16 custom questions (Table 7). Moreover, Table 5 presents the average System Usability Scale (SUS) scores from all participants. Likewise, the average percentage of total satisfaction can be seen in the last row of Table 6, which considers the 7 features included in the table. Note that Table 7 does not report a standard survey or equivalent, where a total or average score would be applicable. Due to the dependency and continuity of these two average scores, we performed a Wilcoxon signed-rank test to compare results. Their corresponding *p*-value is also reported.

Considering all questions included in the self-evaluation, there is a general tendency towards preferring the proposed friction-lockable wrist (LW) over the conventional rotational one (RW). Subjects assigned a higher score to the LW in 82% of the occasions. Only in 6% of the questions, the RW had got more favorable results, while participants considered the performance of both wrists equally useful in 12% of the questions.

Results in Table 5 prove that the LW obtained an SUS score above the average in the literature (i.e., 68), while the average score for the RW is 59.17. The difference between them resulted statistically significant, with a preference for LW. Furthermore, we observed a significant preference of LW over RW in SUS questions (Table 5) regarding control intuitiveness (Q2, Q3, and Q7) and a good integration (Q1, Q5, and Q6).

Previous results are also supported by the outcomes of the device satisfaction, presented in Table 6. The difference in the percentage of the total satisfaction resulted also statistically significant, with a higher value for LW, suggesting a higher degree of acceptability for the proposed system.

In Table 7, questions regarding the perception of a decrease in compensatory movements (Q3, Q11, and Q16), questions concerning the comfortability when performing functional tasks (Q1 and Q10), and questions about the perception of time spent to modify the end-effector configuration (Q5 and Q9), all obtained a significant

improvement. Overall, it is possible to observe a significant difference between prosthetic solutions in 43% of the questions. Results highlight a preference for LW in all cases.

5.2. Subject with limb loss

Even though the results were encouraging from able-bodied subjects, we present additional results from one subject with limb loss for a more direct application and to observe correlation with the previous.

5.2.1. Functional movements. Table 4 shows the wrist usage also for the prosthesis user. The last three columns show, through a picture, the desired approach. Moreover, we report the combination of the DoFs used to orient the end-effector, although it is only qualitative data. Concerning the intact hand (CW), we observed the use of a DoF or a combination of DoFs impossible to reproduce with the RW on 100% of occasions. That highlights the limitations of this commercial solution to recreate natural grasps because of poor functionality. In 88.88% of the cases, the proposed solution (LW) achieves a configuration unreachable by RW. Both prosthetic aids exploit the same approach only for the *cube* at the *middle level*, which appears to be probably the easiest grasping condition.

5.2.2. Self-evaluation. The prosthesis user answered the same surveys to evaluate these perceptions from a real user point of view. Tables 5, 6, and 7 report the prosthesis user's score to each question. In agreement with able-bodied subjects' results, the prosthesis user prefers the proposed system (LW) in all features except for 3 questions of the SUS scale. Considering all 33 questions included in the surveys, the prosthesis user preferred the LW over the RW in 91% of the questions and showed no difference in 9%. We observed a large discrepancy (i.e., 3/4 point difference) in questions regarding easy-to-use (Q2 and Q3 from Table 5), and LW achieved a higher SUS score (52.50) than RW (20.00). While the average device satisfaction (Table 6) for the RW is in the range of *very dissatisfied* (4.76), the LW was evaluated in the range of *satisfied* (61.90), with the maximum punctuation given to grasp naturalness. Table 7 shows a large discordance between prostheses for Q1, Q5, and Q10, which refer to comfortability.

6. Discussion

6.1. Able-bodied subjects

As shown in Figure 9(c), there is no significant difference when both prostheses are active. This suggests that, even if the general execution time favors the RW (Figure 9(a)), the wrist was not actively used during the test (< 20% compared to the LW). This led to different strategies or unnatural body postures to compensate for lack of wrist joint.

Figure 19 shows a sequence of pictures from an able-bodied subject to qualitatively compare grasp naturalness. Underlining the difficulties encountered in extreme cases, where objects shape or their position can hinder the grasp success or require unnatural body configurations, pictures show similarities between the CW and the proposed alternative (LW). Five angles are considered to study body compensations and to present quantitative data regarding this common problem in prosthetics. Among them, we noticed that both elbow F-E and shoulder F-E move on the sagittal plane but in opposite directions. Accordingly, they obtained opposite results in Figure 11. While LW presents a grasp configuration with a more straighten arm, the RW forces the arm to be closer to the torso in order to compensate for the missing DoF at the joint level, which can negatively affect the trunk and shoulder abd/add.

Results from interaction tests highlight the importance of the increased range of motion of the LW at certain conditions. The RW is essentially used for the *cylinder* (almost 100% of wrist activation) regardless of the height. This is proved by the absence of intra-RW differences among heights (Figure 12) and a percentage of active use in each of height condition close to 1/3. Contrarily, the LW is also intentionally used for other objects depending on the height level.

(a) Control wrist (b) Rotational wrist (c) Lockable wrist

Figure 19. Example of compensatory movements performed by an able-bodied subject when grasping the smallest object (card) in the lowest height. A green line highlights the configuration of the arm.

Although results from wrist activation and execution time are encouraging for both prosthetic wrists, they highlight as well possible difficulties in their control, and especially for the RW. In the left side of Figure 12, we observed some involuntary wrist use as RW $\neq 0$ for the *card* or *cube*, where prono/supination was not an intended movement. Indeed, Table 4 shows that all able-bodied participants using the RW performed a top grasp (initial hand configuration of the experiment) for these two objects. In addition, the use of the LW may not be intuitive for able-bodied subjects in some occasions. For example, when participants combine pronation and abd/add. for the grasp of the *cylinder*, we observed a lack of intuitiveness in orienting an external device. This is visible in Figure 13, where the execution time for LW > RW for the *cylinder*, even though it is not significantly larger.

One of the limitations in recording body configuration of the participants is that differences in the setup might have negative effects in the trajectory decided. The gravity compensator (only used for the robotic aids) could be interfering with the natural trajectory and the final configuration. This is visible only in the shoulder abd/add. angle (see Figure 17) at *low*- and *medium levels*, where CW is higher than the prosthetic aids (i.e., more distant from a stand straight up posture). However, as the same setup is used for both robotic systems, their results are comparable.

Generally, results for LW regarding the reduction of compensatory movements are positive. With a more anthropomorphic design, the LW allows subjects to naturally orient the hand in 3 DoF. One example is at the elbow flex/ext. angle (Figure 14), where for the *low-level*, which was the hardest, LW is significantly better than RW. Subjects often used the LW for performing flex/ext. or abd/add. at extreme height conditions, which are missing DoFs in the RW. In addition, even though both prosthetic systems allow hand rotation to grasp the *cylinder* laterally, LW enables the combination of prono/supination with abd/adduction movements. Results from the shoulder abd/add. angle in Figure 17 suggest that these combinations are meaningful to obtain a more natural grasp (closer to CW).

Another interesting effect observed in the results is the compliant condition of the proposed system (LW). In the *medium level*, subjects mostly activate both LW and RW for the grasp of the *cylinder*. The small but significant improvement in the trunk abd/add. angle in Figure 18 suggests that this progress could be attributed to wrist compliant behavior in its *adaptable state*. Finally, results for the trunk flex/ext. angle (see left side of Figure 16) suggest an improved posture of LW, especially for the *card*. This is important because it indicates that even if the SHP (the robotic hand used in all conditions) can adapt towards the object and be useful for the grasp of flat objects, the use of wrist flex/ext. (as occurs only in LW) favors even a more natural grasp.

A natural approach in grasping is fundamental to determine a comfortable user's body posture. Regarding the RW, the execution of 45° rotation requires a more precise control of the wrist than 90°. Note that for the *cylinder*, where both prosthesis aids were used for all conditions, the percentage of grasps including 45° with the LW is always higher or equal than for the RW (see Table 4). This suggests a more intuitive use for the LW or a higher interest in preshaping the joint in many participants. In able-bodied subjects, we observed that the percentage of P-S 45° for the RW is higher at *low*- and *high levels* when grasping the *cylinder*. These results suggest that extreme height levels represent a more challenging condition and subjects usually pay more attention to grasp the object safely. In agreement with the previous, the LW was not intentionally used only at the *medium level* for the *card* and *cube*, probably because a top grasp was preferred for these objects, and the objects were in a height close to subjects' natural workspace.

The assessment of a system acceptance is especially important in the prosthetic and rehabilitation field, as devices become part of users' body. Regarding the self-evaluation surveys, results from able-bodied subjects highlight the potential of the proposed system, which could be a valid alternative for natural grasp approach.

6.2. Subject with limb loss

Due to the lack of biomechanical measures for the prosthesis user, we present a qualitative comparison of grasp naturalness in some particular cases (see Figures 20 and 21). Here, the control case consists of the user' intact arm, which results in hand dexterity differences. This clearly influences

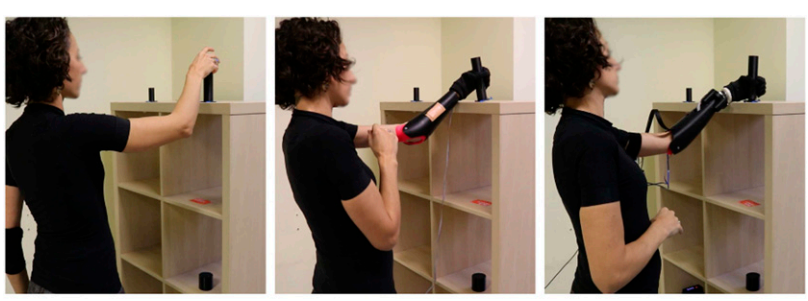

(a) Control wrist (b) Rotational wrist (c) Lockable wrist

Figure 20. Example of body configuration from a prosthesis user grasping a cylinder in the high level height.

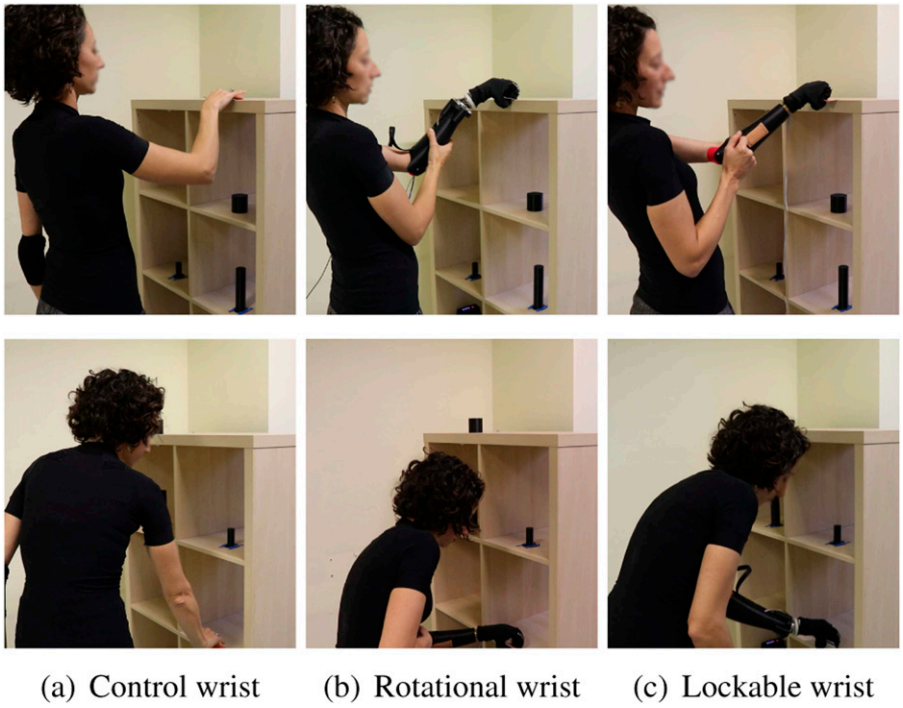

Figure 21. Examples of body configuration from a prosthesis user grasping a card in different heights.

the decision making to approach an object and consequently, defines the whole body posture. Still, the LW showed good functionalities and resulted as an intermediate performant wrist, between the intact arm and the RW characteristics. Similarities between the CW and the LW are observable, and in some cases the combination of DoFs, voluntarily selected by the participant, result in a more natural body configuration. Difficulties encountered with the RW are visible as well, which may lead to a larger cognitive load to grasp the object safely.

Regarding the prosthesis user observations from Table 4, although the design of the LW shows similarities with the control case motions, a reduced number of DoF included is observed. This could occur due to differences in the setup, difficulties in the control due to the weight of the prosthesis, or because of the difficulties encountered to reproduce human dexterity in motion control when using an external robotic device. Only in 33.33% of the occasions, the user performed a completely different grasp approach with the LW compared to the intact arm (control), corresponding always to the *cube*. While the user chooses a lateral approach at 45° with the intact hand, she preferred a top grasp for both prosthetic aids. Due to the availability of the DoFs required at the wrist joint with the LW, differences between the intact and robotic approaches could concern the end-effector capabilities. In fact, in the CW, the participant exploited the dexterity of her intact fingers to hold the object, while in the case of the SHP, the alignment of the palm towards the object is fundamental for a successful grasp.

In regards to the self-evaluation surveys, the difference perceived between both robotic solutions is more evident for the prosthesis user. While in 6% of the 33 questions, able-bodied subjects preferred the rotational wrist (none with statistical significance), the prosthesis user never favored this commercial joint. This effect is also highlighted by the SUS score and the average satisfaction rate (last row in Tables 5 and 6, respectively). Despite the LW SUS score for the prosthesis user (52.50) does not reach the standard value for good acceptance (68—average in the literature), it presents a much higher score than the RW (20.00). We believe this occurs because of its prototype design, far from a lightweight product, which may have a strong effect in real users. The prosthesis user reported free additional comments during the self-evaluation. There, she mentioned the difficulties encountered in intuitively controlling the rotational wrist and especially appreciate the simple use of the lockable wrist to change the configuration of the end-effector as a whole, instead of controlling each DoF individually and in sequence, which is burdensome.

6.2.1. Qualitative observations in ADL. Our musculoskeletal system can accomplish a motor task in many ways by selecting a suitable trajectory and inter-joint coordination (Kim et al., 2014). Purpose-oriented movements, commonly known as Activities of Daily Living, should also be analyzed to evaluate a novel prototype (Murphy et al., 2011). A qualitative comparison among the intact arm and the two prosthetic wrists is shown in Tables 8, 9, and 10. The position of the object or person often is negatively affected by the poor functionality of the RW, increasing the user's discomfort while executing the action. A safer grasp is observed in extreme cases with the LW, where the stability of the object is compromised for the RW (see objects almost

Table 8. Grasping object of different shapes from extreme height cases.

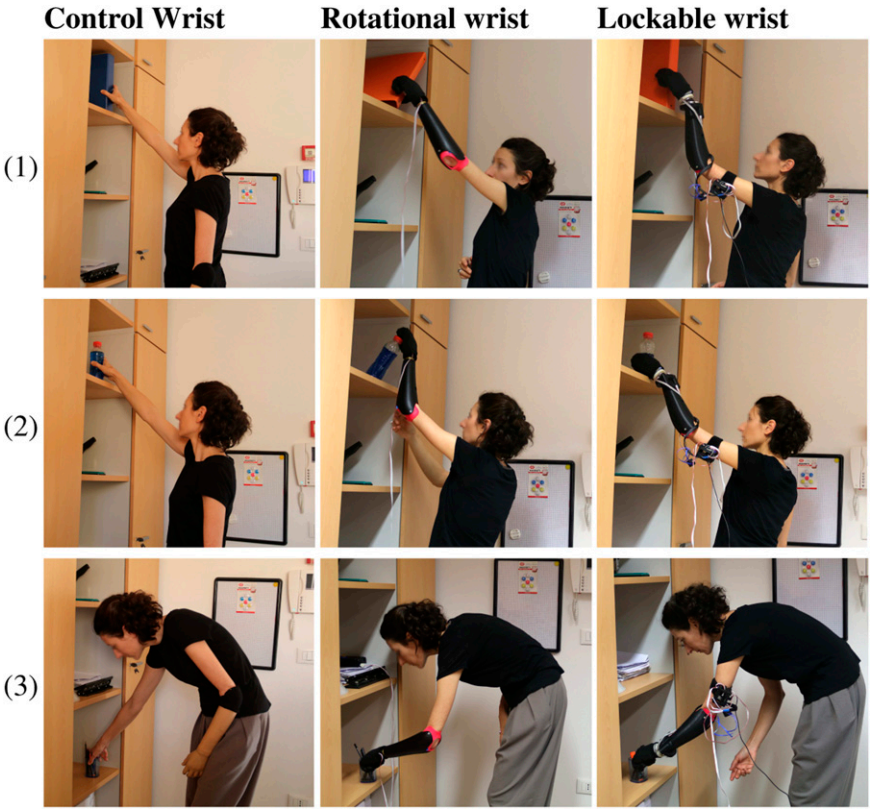

Table 9. Wrist interaction with objects and the environment.

Table 10. Activities of Daily Living: (1) Walking holding hands, (2) pouring water on a cup, and (3) exploring narrow spaces.

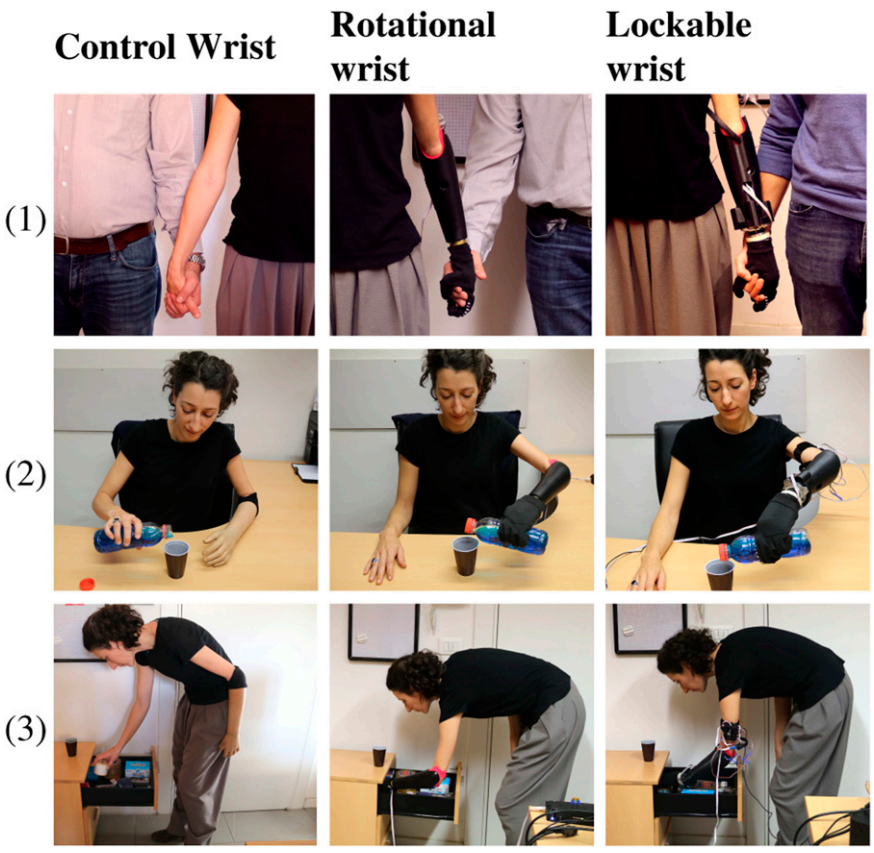

falling in Table 8—*rotational wrist*). A more natural interaction is observed in cases such as the drawer (Table 10 (3)), with the shopping bag or standing up from a chair (Table 9 (2) (3)). Unnatural body positions can be avoided when interacting with objects, such as a suitcase (Table 9 (1)), or other humans. Table 10 (1) shows an example of participants walking holding hands, where the secondary subject is forced to walk behind the prosthesis user only when using the RW, because of its poor adaptability. Overall, our observations suggest an increase in grasp intuitiveness and safety for the LW in its rigid modality, and a more comfortable interaction when behaves adaptable.

7. Conclusions

In this paper, we propose a simple yet useful 3-DoF wrist joint with adaptable and rigid properties. The friction-locking capability enables the adjustment of hand configuration in pre-grasping phases, and the control of the hand and wrist motion independently. Besides, the compliant behavior in F-E and A-A allows a soft interaction with the environment. In addition, this design of 3 DoFs with a simple control strategy offers the unique opportunity to evaluate the effect of an increase in wrist ROM on users' performances.

In this study, our primary focus was not only on stiffness switch (stiff/locked or unlocked/compliant) according to tasks (or grasping phases) but also on providing additional DoFs and examining their usage patterns. Given the return mechanism (due to the compliant interface described in section 3.2.1) to a *Rest position* of the wrist when aiming for a more stable grasp, it often entails a switch in stiffness to secure this hand configuration during the pre-grasping phase. Considering the scope of this study and the numerous research questions addressed, we focused on body configurations related to various wrists, objects, and height levels, instead of assessing intermediate stiffness values and their potential, which the authors anticipate exploring in the future. Moreover, it is important to note that our control scheme, while providing discrete control between wrist and hand, also allows for proportional control of wrist rotation in RW. However, the rapid muscle activation required for entering to the wrist joint state can limit the precision of human muscle control afterward. Furthermore, the limited range for full locking in the LW can hinder the ability to finely adjust its stiffness or friction to intermediate levels. If fine-grained control is a primary requirement, an alternative myoelectric control method would need to be proposed in the future to allow for a more intuitive use of the system (Capsi-Morales et al., 2020).

Results evidence the feasibility of the prototype, its enhanced performance, and present the first impression of the participants. Experimental results from functional tasks proved a significantly larger active usage of the lockable wrist (LW) than a conventional rotational wrist (RW). A substantial increase in the usage of the LW occurred in extreme height conditions where subjects perform F-E, A-A, or a combination of the previous with P-S to better approach the target objects. Note that those wrist configurations are unavailable for the rotational wrist. Moreover, the LW use did not compromise the time execution of the overall prosthesis (both systems around 19s), hence improving only wrist functionality. Concerning compensatory movements, interaction tests proved that when there was significance, results always favor the LW over the RW, also showing a closer resemblance to the control wrist (CW). The self-evaluation surveys reported a significant preference of the LW in questions concerning control intuitiveness, good integration, comfortability and perception of a decrease of compensatory movements, and performance speed. The average satisfaction and SUS scores also resulted significantly higher for the LW, suggesting the acceptance of the proposed system. A similar tendency is observed in prosthesis user's answers. Finally, a preliminary evaluation in ADL suggested enlarged capabilities regarding intuitiveness, grasp safety, and softer interaction. While the data from experiment **(2)** could not be subjected to statistical analysis due to participant limitations and missing body compensation quantification, it offers qualitative insights into the real user experience in more challenging and relevant scenarios than in the controlled functional testing of experiment **(1)**. Able-bodied participants were not included in the second experiment due to difficulties in collecting their data in a less constrained environment, mainly because of the use of a bypass and gravity compensator, which already affects their "natural" use of robotics in ADL.

Even though the lockable wrist is designed to permit its orientation through the environment and/or the intact hand, the subjects modified the wrist joint with the assistance of the intact hand during the experiments. The passive modification of the end-effector orientation through the environment is not trivial and could negatively affect the execution time. However, this feature could be especially convenient for bilateral amputees.

The limitations of the study include the lack of control over shelf heights during the experiment in relation to participant heights, potentially impacting wrist usage variations. It is worth noting that more recent and comprehensive functional assessments for patients, such as ACMC (Hermansson et al., 2005), AM-ULA (Resnik et al., 2013), and CYBATHLON tasks (Jaeger et al., 2023), have made efforts to incorporate various grasping and releasing scenarios in different configurations. This is intended to address the previously overlooked aspect of wrist motion during grasping or standard functional assessments. Furthermore, the study could benefit from a more diverse set of objects, which was limited by the experiment duration. We hope that our study can draw attention to the need for standard assessments in more complex scenarios, prompting the development of controlled tests with comparable setups.

Despite the limitation of involving a single prosthesis user, we believe that the statistical analysis of able-bodied participants' data still provides valuable insights into the significance of wrist DoFs and underscores the need for more comprehensive systems in achieving dexterous manipulation. Due to the encouraging results, future works will encompass an extensive evaluation with a larger group of prosthesis users and point towards a more compact and light design with a larger range of motion. Future research endeavors should present a more refined joint design with variable impedance, where a comprehensive characterization of the friction and impedance will be a central focus to further advance the field. For precise control of wrist stiffness levels or simultaneous control of both wrist and hand properties, a more advanced myoelectric control method would need to be proposed in the future.

8. Appendix

Due to the physical inter-subject differences and possibly not exact starting position relative to the height differences in subjects, we considered the average angle from a window (3 samples) right after the successful grasp event (dashed red line in Figure 22), where desired/needed subject body configuration is stable. We defined the successful grasp event at the instant with the 50% hand total closure from the last complete closure executed for that experimental condition.

An example of the data obtained from Xsens and the motor encoders is presented in Figure 22. The reference configuration of the prosthetic hand and its division into two phases by a red dashed line is shown in the first row. The first phase represents the reaching and grasping of the action, while the second represents the transport and release phase. In the left column, the data from the three wrists is synchronized by the middle event (successful grasp). The x-axis represents the execution time with a marker that indicates the starting and the ending of the action. The rest of the rows represent the 5 joint angles selected to study the range of compensatory movements. This column allows the visualization of the time needed to reach the object and perform the task. On the other hand, in the right column, the data is almost overlapped. There, signals are synchronized by the duration of each phase over the percentage of completion. Therefore, while the left column normalizes the time, giving t = 0 at the successful grasp event, the right column stretches the signal until the three wrists get a common duration. The right column facilitates the understanding of the similarities and differences between wrist use and body angles.

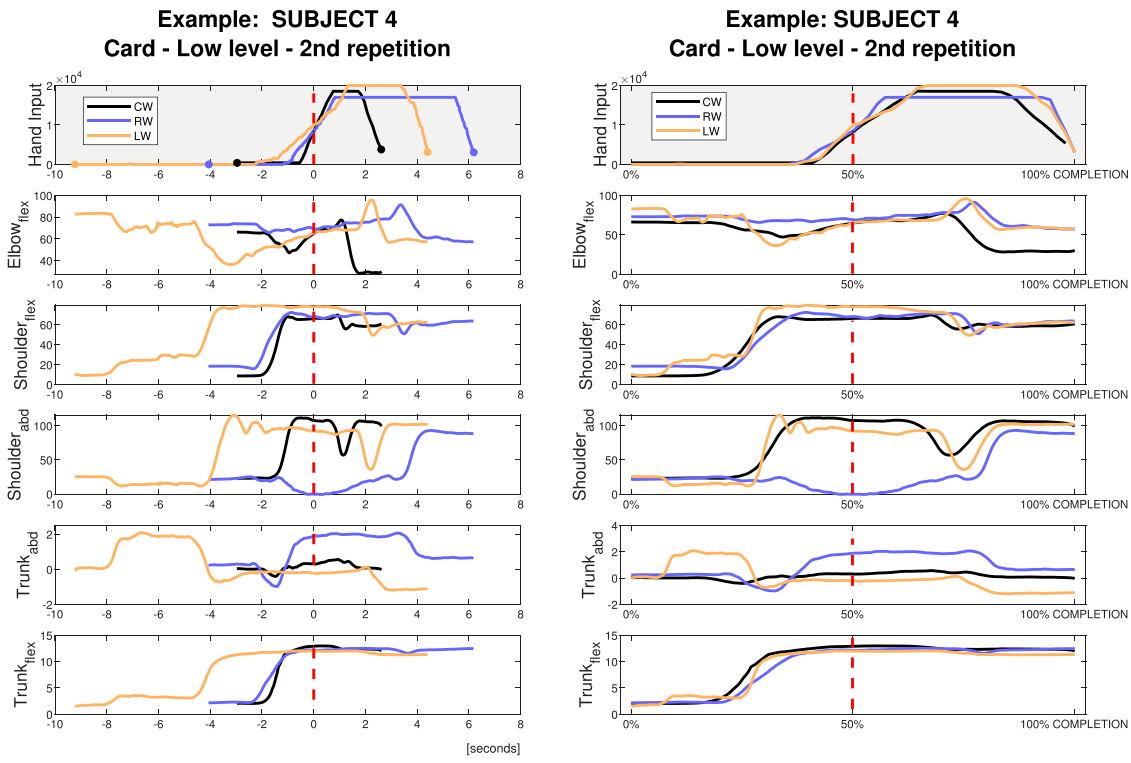

Figure 22. Example of compensatory movements from a subject in a particular case: grasping the card at the low-level height (2nd repetition). The part before the dashed red line refers to the reaching and grasping phase, while the second part refers to the transport and release phase of the action.

Acknowledgments

The authors warmly thank Mattia Poggiani and Andrea Di Basco for their valuable help in the realization of the experimental validation and the manufacturing of the system pieces, respectively.

Declaration of conflicting interests

The author(s) declared no potential conflicts of interest with respect to the research, authorship, and/or publication of this article.

Funding

The author(s) disclosed receipt of the following financial support for the research, authorship, and/or publication of this article: This research has received funding from the European Union's Horizon 2020 Research, ERC programme under the Grant Agreement No. 810346 (Natural Bionics). The content of this publication is the sole responsibility of the authors. The European Commission or its services cannot be held responsible for any use that may be made of the information it contains.

ORCID iDs

Patricia Capsi-Morales https://orcid.org/0000-0001-6498-9231
Giorgio Grioli https://orcid.org/0000-0002-5310-2997
Manuel G. Catalano https://orcid.org/0000-0003-1950-6186

References

Alvin JK (2011) Friction locking spherical joint. US Patent 4,741,207. URL: https://patents.google.com/patent/US20130077904A1

Bajaj NM and Dollar AM (2018) Design and preliminary evaluation of a 3-dof powered prosthetic wrist device. In: 2018 7th IEEE International conference on biomedical robotics and biomechatronics (Biorob), pp. 119–125. IEEE.

Bajaj NM, Spiers AJ and Dollar AM (2015) State of the art in prosthetic wrists: commercial and research devices. In: Rehabilitation robotics (ICORR), 2015 IEEE international conference on, pp. 331–338. IEEE.

Bajaj NM, Spiers AJ and Dollar AM (2019) State of the art in artificial wrists: a review of prosthetic and robotic wrist design. *IEEE Transactions on Robotics* 35(1): 261–277.

Belter JT, Segil JL, Dollar AM, et al. (2013) Mechanical design and performance specifications of anthropomorphic prosthetic hands: a review. *Journal of Rehabilitation Research and Development* 50(5): 599–618.

Bertels T, Schmalz T and Ludwigs E (2009) Objectifying the functional advantages of prosthetic wrist flexion. *JPO: Journal of Prosthetics and Orthotics* 21(2): 74–78.

Brown E, Rodenberg N, Amend J, et al. (2010) Universal robotic gripper based on the jamming of granular material. *Proceedings of the National Academy of Sciences* 107(44): 18809–18814.

Cappello L, D'Accolti D, Gherardini M, et al. (2022) A 2-degree-of-freedom quasi-passive prosthetic wrist with two levels of compliance. *IEEE Robotics and Automation Letters* 8: 1231–1238.

Capsi-Morales P, Piazza C, Catalano MG, et al. (2020) Exploring stiffness modulation in prosthetic hands and its perceived function in manipulation and social interaction. *Frontiers in Neurorobotics* 14: 33.

Capsi-Morales P, Piazza C, Catalano MG, et al. (2021) Comparison between rigid and soft poly-articulated prosthetic hands in non-expert myo-electric users shows advantages of soft robotics. *Scientific Reports* 11(1): 23952.

Capsi-Morales P, Barbarossa M, Piazza C, et al. (2022) Friction-lockable prosthetic wrist. Italian Patent application, 102021000008261.

Carey SL, Jason Highsmith M, Maitland ME, et al. (2008) Compensatory movements of transradial prosthesis users during common tasks. *Clinical Biomechanics* 23(9): 1128–1135.

Chen C, Yu Y, Sheng X, et al. (2023) Mapping individual motor unit activity to continuous three-dof wrist torques: perspectives for myoelectric control. *IEEE Transactions on Neural Systems and Rehabilitation Engineering: A Publication of the IEEE Engineering in Medicine and Biology Society* 31: 1807–1815.

Cipriani C, Controzzi M and Carrozza MC (2011) The smarthand transradial prosthesis. *Journal of NeuroEngineering and Rehabilitation* 8(1): 29.

Controzzi M, Cipriani C and Carrozza MC (2014) Design of artificial hands: a review. In *The Human Hand as an Inspiration for Robot Hand Development*. Springer, 219–246.

Cutkosky MR (1989) On grasp choice, grasp models, and the design of hands for manufacturing tasks. *IEEE Transactions on Robotics and Automation* 5(3): 269–279.

Dalley SA, Wiste TE, Withrow TJ, et al. (2009) Design of a multifunctional anthropomorphic prosthetic hand with extrinsic actuation. *IEEE/ASME transactions on mechatronics* 14(6): 699–706.

Davidson J (2002) A survey of the satisfaction of upper limb amputees with their prostheses, their lifestyles, and their abilities. *Journal of Hand Therapy: Official Journal of the American Society of Hand Therapists* 15(1): 62–70.

de los Reyes-Guzmán A, Dimbwadyo-Terrer I, Trincado-Alonso F, et al. (2014) Quantitative assessment based on kinematic measures of functional impairments during upper extremity movements: a review. *Clinical Biomechanics* 29(7): 719–727.

Deijs M, Bongers R, Ringeling-van Leusen N, et al. (2016) Flexible and static wrist units in upper limb prosthesis users: functionality scores, user satisfaction and compensatory movements. *Journal of NeuroEngineering and Rehabilitation* 13(1): 1–13.

Della Santina C, Piazza C, Gasparri GM, et al. (2017) The quest for natural machine motion: an open platform to fast-prototyping articulated soft robots. *IEEE Robotics and Automation Magazine* 24(1): 48–56.

Demofonti A, Carpino G, Tagliamonte NL, et al. (2023) Design of a modular and compliant wrist module for upper limb prosthetics. *The Anatomical Record* 306(4): 764–776.

Fite KB, Withrow TJ, Shen X, et al. (2008) A gas-actuated anthropomorphic prosthesis for transhumeral amputees. *IEEE Transactions on Robotics* 24(1): 159–169.

Fitts PM (1954) The information capacity of the human motor system in controlling the amplitude of movement. *Journal of Experimental Psychology* 47(6): 381–391.

Gambrell CR (2008) Overuse syndrome and the unilateral upper limb amputee: consequences and prevention. *JPO: Journal of Prosthetics and Orthotics* 20(3): 126–132.

Godfrey SB, Zhao KD, Theuer A, et al. (2018) The softhand pro: functional evaluation of a novel, flexible, and robust myoelectric prosthesis. *PLoS One* 13(10): e0205653.

Hermansson LM, Fisher AG, Bernspång B, et al. (2005) Assessment of capacity for myoelectric control: a new rasch-built measure of prosthetic hand control. *Journal of Rehabilitation Medicine* 37(3): 166–171.

Jacobs R (1993) The addition of a flexible wrist unit to enhance prosthetic function. In: Myoelectric Symposium. Duke University*Myoelectric Symposium*.

Jaeger L, Baptista RS, Basla C, et al. (2023) How the cybathlon competition has advanced assistive technologies. *Annual Review of Control, Robotics, and Autonomous Systems* 6: 447–476.

Jiang N, Vest-Nielsen JL, Muceli S, et al. (2012) Emg-based simultaneous and proportional estimation of wrist/hand kinematics in uni-lateral trans-radial amputees. *Journal of NeuroEngineering and Rehabilitation* 9(1): 42.

Jiang N, Rehbaum H, Vujaklija I, et al. (2014) Intuitive, online, simultaneous, and proportional myoelectric control over two degrees-of-freedom in upper limb amputees. *IEEE Transactions on Neural Systems and Rehabilitation Engineering: A Publication of the IEEE Engineering in Medicine and Biology Society* 22(3): 501–510.

Kidd PS, McCoy C and Steenbergen L (2000) Repetitive strain injuries in youth. *Journal of the American Academy of Nurse Practitioners* 12(10): 413–426.

Kim K, Song WK, Lee J, et al. (2014) Kinematic analysis of upper extremity movement during drinking in hemiplegic subjects. *Clinical Biomechanics* 29(3): 248–256.

Kyberd PJ (2011) The influence of control format and hand design in single axis myoelectric hands: assessment of functionality of prosthetic hands using the southampton hand assessment procedure. *Prosthetics and Orthotics International* 35(3): 285–293.

Kyberd PJ (2012) The influence of passive wrist joints on the functionality of prosthetic hands. *Prosthetics and Orthotics International* 36(1): 33–38.

Lee G, Hong GY and Choi Y (2021) Tendon-driven compliant prosthetic wrist consisting of three rows based on the concept of tensegrity structure. *IEEE Robotics and Automation Letters* 6(2): 3956–3963.

Lenzi T, Lipsey J and Sensinger JW (2016) The ric arm—a small anthropomorphic transhumeral prosthesis. *IEEE* 21(6): 2660–2671.

Metzger AJ, Dromerick AW, Holley RJ, et al. (2012) Characterization of compensatory trunk movements during prosthetic

upper limb reaching tasks. *Archives of Physical Medicine and Rehabilitation* 93(11): 2029–2034.

Montagnani F, Controzzi M and Cipriani C (2013) Preliminary design and development of a two degrees of freedom passive compliant prosthetic wrist with switchable stiffness. In: Robotics and biomimetics (ROBIO), 2013 IEEE international conference on, pp. 310–315. IEEE.

Montagnani F, Controzzi M and Cipriani C (2015) Is it finger or wrist dexterity that is missing in current hand prostheses? *IEEE Transactions on Neural Systems and Rehabilitation Engineering: A Publication of the IEEE Engineering in Medicine and Biology Society* 23(4): 600–609.

Montagnani F, Smit G, Controzzi M, et al. (2017) A passive wrist with switchable stiffness for a body-powered hydraulically actuated hand prosthesis. In: Rehabilitation robotics (ICORR), 2017 international conference on, pp. 1197–1202. IEEE.

Moser N, O'Malley MK and Erwin A (2020) Importance of wrist movement direction in performing activities of daily living efficiently. In: 2020 42nd annual international conference of the IEEE engineering in medicine & biology society (EMBC), pp. 3174–3177. IEEE.

Murphy MA, Willén C and Sunnerhagen KS (2011) Kinematic variables quantifying upper-extremity performance after stroke during reaching and drinking from a glass. *Neurorehabilitation and Neural Repair* 25(1): 71–80.

Nowak M, Vujaklija I, Sturma A, et al. (2022) Simultaneous and proportional real-time myocontrol of up to three degrees of freedom of the wrist and hand. *IEEE Transactions on Biomedical Engineering* 70(2): 459–469.

Oskoei MA and Hu H (2007) Myoelectric control systems—a survey. *Biomedical Signal Processing and Control* 2(4): 275–294.

Østlie K, Franklin RJ, Skjeldal OH, et al. (2011) Musculoskeletal pain and overuse syndromes in adult acquired major upper-limb amputees. *Archives of Physical Medicine and Rehabilitation* 92(12): 1967–1973.

Palpacelli M, Carbonari L and Palmieri G (2014) A lockable spherical joint for robotic applications. In: Mechatronic and embedded systems and applications (MESA), 2014 IEEE/ASME 10th international conference on, pp. 1–6. IEEE.

Petersen B (2008) Preliminary feedback from field trial users of the motion control multi-flex wrist. In: Myoelectric Symposium. Duke University.

Piazza C, Rossi M, Catalano MG, et al. (2020) Evaluation of a simultaneous myoelectric control strategy for a multi-dof transradial prosthesis. *IEEE Transactions on Neural Systems and Rehabilitation Engineering* 28(10): 2286–2295.

Resnik L, Adams L, Borgia M, et al. (2013) Development and evaluation of the activities measure for upper limb amputees. *Archives of Physical Medicine and Rehabilitation* 94(3): 488–494.

Schultz AE and Kuiken TA (2011) Neural interfaces for control of upper limb prostheses: the state of the art and future possibilities. *PM & R: The Journal of Injury, Function, and Rehabilitation* 3(1): 55–67.

Sears HH, Iversen E, Archer S, et al. (2005) Evaluation studies of new electric terminal devices. *Myoelectric Symposium*.

Smith LH, Kuiken TA and Hargrove LJ (2015) Evaluation of linear regression simultaneous myoelectric control using intramuscular emg. *IEEE Transactions on Biomedical Engineering* 63(4): 737–746.

Stavdahl Ø (2002) *Optimal Wrist Prosthesis Kinematics: Three-Dimensional Rotation Statistics and Parameter Estimation*. PhD Thesis, Institutt for Teknisk Kybernetikk.

Telleria MJ, Panas R and Culpepper ML (2009) *Mr Fluid Activated Spherical Joint for Precision Orientation Control*. In: 24th American society for precision engineering annual meeting. ASPE.

Todorov E (2004) Optimality principles in sensorimotor control. *Nature Neuroscience* 7(9): 907–915.

Weir R, Mitchell M, Clark S, et al. (2008) The intrinsic hand–a 22 degree-of-freedom artificial hand-wrist replacement. In: Myoelectric Symposium. Duke University.

Young AJ, Smith LH, Rouse EJ, et al. (2013) Classification of simultaneous movements using surface EMG pattern recognition. *IEEE Transactions on Biomedical Engineering* 60(5): 1250–1258.

Zinck AL (2008) *Investigation of Compensatory Movements in Prosthesis Users and the Design of a Novel Wrist*. PhD Thesis, University of New Brunswick, Department of Mechanical Engineering.